ceramics

MDPI

Article

Non-Invasive On-site pXRF Analysis of Coloring Agents, Marks and Enamels of Qing imperial and non-imperial porcelain

Philippe Colomban [1,*], Gulsu Simsek Franci [2], Jacques Burlot [1], Xavier Gallet [3], Bing Zhao [4], Jean- Baptiste Clais[5] and Claire Delery [6]

[1] MONARIS UMR8233, Sorbonne Université, CNRS, 4 Place Jussieu, 75005 Paris, France, jacques.burlot@sorbonne-universite.fr
[2] Surface Science and Technology Center (KUYTAM), College of Sciences, Rumelifeneri Campus, Koç University, 34450 Istanbul, Turkey; gusimsek@ku.edu.tr or gulsu.simsek@gmail.com
[3] Musée de l'Homme, Musée National d'Histoire Naturelle, Paris, France, xavier.gallet@mnhn.fr
[4] CNRS, CRCAO, UMR8155, Collège de France, 75005, Paris, France, bing.zhao@college-de-france.fr
[5] Département des objets d'art, Musée du Louvre, quai François Mitterrand, 75001 Paris, France; jean-baptiste.clais@louvre.fr
[4] Musée national des arts asiatiques, Guimet, Paris, France, claire.delery@guimet.fr
* Correspondence: philippe.colomban@sorbonne-universite.fr or philippe.colomban@upmc.fr

Abstract: On-site pXRF analysis in various French museums (Louvre, Musée national des Arts asiatiques-Guimet, Paris) of porcelains decorated with painted enamels from the Qing Dynasty, in particular porcelains bearing an imperial mark, identifies the types of enamels/glazes, the ions and coloring phases or opacifier. The study of the elements associated with cobalt (nickel, manganese, arsenic, etc.) and of the impurities of the silicate matrix (yttrium, rubidium and strontium) differentiates the use of 'Chinese/Asian' raw materials from ones imported from Europe by the initiative of the Jesuit missionaries present at the Court (Forbidden City). Particular attention is paid to the analysis of the blue color of the marks and to the elements associated with the use of gold or copper nanoparticles as well as the compositions of the pyrochlore phases (tin yellow, Naples yellow). The comparison is extended to pXRF and Raman microspectroscopy measurements previously made on other Qing imperial porcelains as well as Cantonese productions (on porcelain or metal) from different Swiss and French museums and blue-and-white wares of the Ming and Yuan Dynasties (archaeological and private collections).

Keywords: pXRF; porcelain; enamels; glaze; cobalt ; arsenic ; gold ; mark ; pigments ; opacifier ; blue: yellow; green; rose; red; white.

1. Introduction

As in Japan at the end of the 16th century at the Court of the Nabeshima clan in Arita (Kyushu, Japan, beginning of the Edo period (1603-1868)),[1] the Jesuits residing in the Imperial Forbidden City of Beijing during the reign of the Emperor Kangxi (1662-1722) and his successors Yongzheng (1723-1735) and Qianlong (1736-1795) played a decisive role in the transfer of European enameling and painting know-how to Asian craftsmen. Chinese archives and Jesuit correspondence bear witness to the demands of the emperors, the difficulties and successes in setting up enameling (1693) and glass

production (1696) workshops in the Forbidden City, the arrival of European experts, Jesuits or not (1698 and after) and the importation of ingredients to obtain a palette of colors, opaque and mixable (1715-1722) allowing the realization of sophisticated realistic enamel decorations rivaling oil painting.[2-14] Such enamel decorations had been made in France since the middle of the 17th century on metalware.[15] The Chinese documents also testify to numerous exchanges of information but also of craftsmen between the workshops of the Forbidden City and the imperial kilns of Jingdezhen where the porcelain 'supports' were produced, but also with the other, 'private' or official kilns of Jingdezhen and the enameling workshops, on porcelain or on metal, of Canton.[11,13,14]

Let us recall that the production of porcelain in Europe, if we except the very particular case of the hybrid porcelain of Medici (1575-1587)[16], dates back to ~1670 for the synthesis of soft-paste porcelain (in a way a fritware inspired by ceramics from 'Iznik') in Rouen, then Saint-Cloud in France, and Fulham in the United Kingdom)[17] and ~1710 for the 'true' china, i.e. a mullite-based hard-paste porcelain, in Meissen (Saxony)[18], the latter being very close to Chinese productions because using similar rocks for the paste (kaolin and kaolin-like rocks, pegmatite, quartz, etc.)[19-21]. The enamels of soft-paste porcelain, with a lead-based flux therefore fired at low temperature (muffle kiln, ~700 to 1000°C), heirs to the know-how of majolica enamels, Limoges enamels (metalware) and enamels on glass allow a wide range of colors.[22-25] On the contrary, hard-paste porcelain glazes fired at a much higher temperature (~1280°C in China, ~1380°C in Europe) only offer a reduced palette, rather similar to that of stained glass.[22,26,27,28] Indeed the realization of enamels imposes on this layer of thin glass deposited on an often opaque and non-porous substrate, particular constraints: its low thickness, a few tens to hundred(s) of microns, imposes a significant concentration in coloring agent(s); a 'white' phase, the opacifier usually needs to be added to 'brighten' the color.[24,30,31] The realization of the decoration on a non-porous support (and not on an unfired (green body) or biscuit (porous) paste (first firing around 950°C)) such as glass, metal or fired porcelain requires the use of mediums particular (essences, oils, glues, resins) and not water as used to drawn a porous substrate. In the end, the colored areas must be preserved during firing (no interdiffusion or 'burrs'), presenting after firing the shine and the desired thickness without defects (flaking, cracking) which determines the constraints of viscosity, thermal expansion, melting temperature, etc.[32]

The techniques for coloring a layer of glass implement three types of coloring agents: i) ions exhibiting absorption in the visible, i.e. having incomplete 3d electronic layers (transition metals) or 4f (rare earths) dissolved in the silicate network; ii) nanoparticles absorbing in the visible, i.e. low-gap (metals such as gold, copper or silver and semiconductors such as CdS and CdSe); iii) pigments colored by the means mentioned above prepared separately and dispersed in the silicate powder before firing or forming on cooling from the silicate melt oversaturated in certain elements.[23-25,29] The technical literature shows that for the same visual aspect several preparation techniques are possible. [23-25,29,30,33] Since longtime most of colored glaze and enamels are prepared from two mixtures: one enriched in coloring agent(s) (e.g. smalt, the cobalt-rich potash

glass that contain up to ~20 %wt CoO [33]), called *anima* in ancient recipes [34] and a colorless mixture (*corpo*) that will form the silicate matrix [23,26], convenient to control the melting temperature, the thermal expansion, the viscosity, etc. [24,32]. The first mixture, and sometimes the second one, is prepared by glass technique: raw materials are melted in a crucible and the melt is poured in water what leads reduces the glass to powder called frit. Typically the content of coloring phase range between less than 0.5 wt% (e.g., CoO or Au°) up to 5-10 wt% (e.g., Fe_2O_3).

The objects with sophisticated decorations made for the Emperors of China are among the most appreciated ceramic masterpieces, particularly in Asia, and their value rivals that of many paintings by Western great masters. Also no sampling is possible and even transport to a laboratory is rarely possible given the costs of packaging and insurance. The analysis must be done in the secure place of storage or exhibition. Our previous works [15,17,18,35-40] have shown that the combination of mobile X-ray fluorescence (pXRF) instruments (information on the chemical elements present) and mobile Raman microspectroscopy set-up (information on the 'molecular' structure, i.e. on the crystalline phases or amorphous) identified the coloring agents and phases present in the glazes and enamels, thus making it possible to compare the raw materials and techniques for preparing, laying and firing the decorations despite the impossibility of observing the stratigraphy as is possible on a fracture or a shard.[41,42] However, for a perfect interpretation of the results, the study by the same instruments and other more powerful ones (in particular SEM-EDS, XRD, PIXE and PIGE), in the laboratory of similar shards is essential.

In this work we will compare a selection of enameled objects, mainly porcelain, belonging to the collections of the musée national des Arts asiatiques-Guimet (mnaa-g) and the musée du Louvre bearing imperial marks and/or stylistically attributed to the reigns of Kangxi, Yongzheng and Qianlong. These objects have already been analyzed by Raman microspectroscopy [38-40,43]. Additional artifacts assigned to second part of 19th century are studied. We will then compare the results with those obtained on similar pieces from the Chinese museum of the Château de Fontainebleau [35,43] and the Swiss museums of the Baur Foundation and the Ariana museum [36,37] as well as with sets of Chinese and Vietnamese ceramics from previous dynasties (Ming and Yuan) [44-46]. Such a set of exceptional Qing artifacts has never been analyzed or discussed. Except a recent study of imperial teapots [47], previous XRF studies are related to shards [48-52], and more common pieces [53-56]. The number of pieces considered is around 60 for Qing objects, and several dozen for objects from Europe [see reference [18] and references herein) or from earlier Chinese (and Vietnamese) periods [33-35]. A few comparable shards have also been analyzed in depth at the laboratory using many techniques.[41,42,57]

The questions we will try to answer are the identification of the use of raw materials and/or European recipes in the objects and the evolution of technologies during the 18th and 19th centuries, the comparison between productions in Beijing and in Canton, for the Emperor, the Chinese market and export (*porcelaines de commande* / armorial ex-

port porcelain)[41], the similarities and differences between enamels on porcelain and on metal and the comparison with similar productions made simultaneously in Europe.

2. Materials and Methods

2.1. Artifacts

The analyzed objects are shown in Figure 1 and Table 1 summarizes information. The pieces have been selected to represent the period when technical innovations could be linked to the presence of the Jesuits.[3-5,38,58] To this were added 19th century porcelains which may have been made after 1850, i.e. using as coloring agents chemically purified raw materials and not 'simple' minerals empirically selected and partially transformed by roasting and/or or acid attack [33,59]. For comparison some Canton metalware and Yixing stoneware previously analyzed are included [38,39].

Figure 1. View of analyzed parts. Existing marks are presented. The allocated production period is specified (see Table 1 for details).

The date assignment is quite accurate and reliable for some pieces [35-40,43] and many artifacts have been recently discussed [60,61]. An overview of Qing Dynasty enamelware productions can be found in references [62-69].

Table 1. Studied corpus.

Museum	Inventory number	Description	Remarks	Date	Type (expected kiln)	Refs
Louvre	R1041	porcelain	Similar cup at different museums	1722-35		43
	R1175	porcelain	English family coat of arms	1735		43
	R1177	porcelain		1735		43
	R1045	porcelain	Similar cup at Rijksmuseum	1730-45		43
	TH487	porcelain		1730-35		43
	R1048	porcelain		1740-60		43
	R958	metalware		1730-96	Canton	39
	R975	metalware		1730-96	Canton	39
Guimet	G5687	porcelain		middle 17th c.	*doucai* (Jingdezhen) Private kiln	
	G5696	porcelain	Kangxi mark	~1700	*doucai* (Jingdezhen)	38
	G3361	porcelain	Kangxi mark	~1700	*Famille rose* (Jingdezhen)	38
	G5250	porcelain	Kangxi mark	1715-22	*falangcai* (Forbbiden City)	38,60
	G913	porcelain	Yongzheng mark	1723-35	*falangcai* (imperial Jingdezhen)	38
	G4806	porcelain	Yongzheng mark	1723-35	*falangcai* (imperial Jingdezhen)	38
	MG3668	stoneware		2nd half 18th c.	Yixing (private kiln)	38
	G823	porcelain		18th c.		
	MG8062	stoneware		19th c.	Yixing (private kiln)	38
	G5615	porcelain		19th c.		
	G4939	porcelain		19th c.		
	MG907	porcelain		19th c.		
	G2789	porcelain		19th c.		
	G2890	porcelain		19th c.?		

Présentation stylistiques des pieces, intérêt, pieces similaires dans des catalogues-ref et musées

2.2. Method

The procedure has been described in previous articles in details.[15,18,36,37] X-ray fluorescence analysis was performed on site using a portable ELIO instrument. The

set-up included a miniature X-ray tube system with a Rh anode, a ~1 mm^2 collimator) and a large-area Silicon Drift Detector with an energy resolution of <140 eV for Mn Kα, an energy range of detection from 1.3 keV (in air) to 43 keV. The working distance is 1.4 cm. We measured the standard DRN to validate our approach. Depending on the object, the measurement was carried out by positioning the instrument on the top or on the side. Perfect perpendicularity to the area measured is searched. Measurements were carried out in the point mode with an acquisition time of 150 s, using a tube voltage of 50 kV and a current of 80 μA. No filter was used between the X-ray tube and the sample. The analysis depth during the measurement of the enamel was estimated from the Beer–Lambert law (analysis depth, defined as the thickness of the top layer from which comes 90% of the fluorescence)[70] to be close to 6 μm at Si K_α, 170 μm at Cu K_α, 300 μm at Au L_α, and 3 mm at Sn K_α. Within the resolution of the pXRF instrument, the Fe K_β peak and the Co K_α peak corresponding to the blue color are located in the same energy range and fitting is required to extract relative contriution of each.

The data fitting procedure has been already used in previous papers.[36,37] After recording the raw data with ELIO, the spectra files were opened in the Artax 7.4.0.0 (Bruker, AXS GmbH, Karlsruhe, Germany) software. For the data treatment process, the studied objects were considered infinitely thick samples. Before evaluating the analysis data, all of the spectra were imported, and a new method file was created via "Method Editor" of Artax for an applied voltage of 50 kV and current of 80 μA. The corresponding major (e.g., K, Ca), minor (e.g., Fe, Ti, Co, As), and trace elements (e.g., Ag, Bi…) were added to the Periodic Table. For the correction, escape and background options were selected in the Method Editor, and 10 cycles of iteration were selected starting from 0.5 keV to 45 keV. The deconvolution method, Bayes, was applied to export the data table. The net area was calculated under the peak at the characteristic energy of each element selected in the periodic table, and the counts of the major, minor, and trace elements were determined in the colored areas (white, red, yellow, orange, blue, green, and black). Normalization with respect to the signal Si or Co or Rh was made for the comparison of certain elements, in particular for the data coming from different measurement campaigns. Before plotting the scatter diagrams, the net areas of each element were normalized by the number of XRF photons derived from the elastic peak of the X-ray tube of rhodium. Then, these normalized data were plotted in the ternary scattering plots drawn for the interpretation and discussion of the results with the software Statistica 13.5.0.17 (TIBCO Software Inc., Palo Alto, CA, USA).

3. Results

3.1. Information that can be obtained from the XRF fingerprint

The most representative spectra have been selected to be presented in the Figures 2 to 4, all the results being given in a Table. A first set of information is evident from the observation of the spectra in the characteristic energy ranges of the elements present, namely 0.1 to 20 keV for the main elements (Figures 2-4) and 25-32 keV for the tin, antimony and silver (Figures 2 and 4).

The presence of lead causes the spectra to be dominated by the peaks of the Lα, Lβ, and Lγ transitions plus other minor contributions (example yellow zone of bowl G5696, Figure 2), these peaks remain significant even when the presence of lead results from the pollution of the glaze surface during overglaze firing (G5696 blue, Figure 2). Figure 2 highlights the three technical solutions to obtain colors ranging from yellow to green, the traditional Chinese recipe with iron ions (bowl *wucai* G5696 yellow) [19], the addition of tin-antimony (bowl *falangcai* G5250, tin yellow and Naples yellow pyrochlore) or the

'simple' tin yellow (G5250 green), also easily differentiated by Raman microspectroscopy [15,23,28,34,35-37,41,71-79]. Comparison of the spectrum recorded on the blue decoration of the G5250 *falangcai* bowl with that of the mark of the 5696 *wucai* bowl clearly shows the use of different sources of cobalt, the manganese-rich 'Asian cobalt' typical of (late) Yuan productions, Ming productions, and production from the reign of Kangxi before ~1700 [33,80-96] and the 'European cobalt' rich in arsenic for here the *falangcai* bowl G5250, as has already been highlighted for this object by Raman microscopy [38-40]. An almost identical signature is observed for the *falangcai* bowl G823, and for the Yixing teapot MG3668 (Figure 3) for which the surface pollution of the cover by the overglaze lead is much lower. On the other hand, for the vase G5687 *'Famille verte*', typical of a production prior to 1700, as expected we find the use of 'Asian cobalt' rich in manganese. On the other hand, the spectrum of bowl MG907 shows an intense cobalt peak, much more intense than that of the associated elements such as iron and manganese. This is characteristic of the use as a source of cobalt of a 'refined' chemical product, salts or oxide and therefore of a production after ~1850, in accordance with its attribution on stylistic (visual) criteria of the decoration (19th or after).

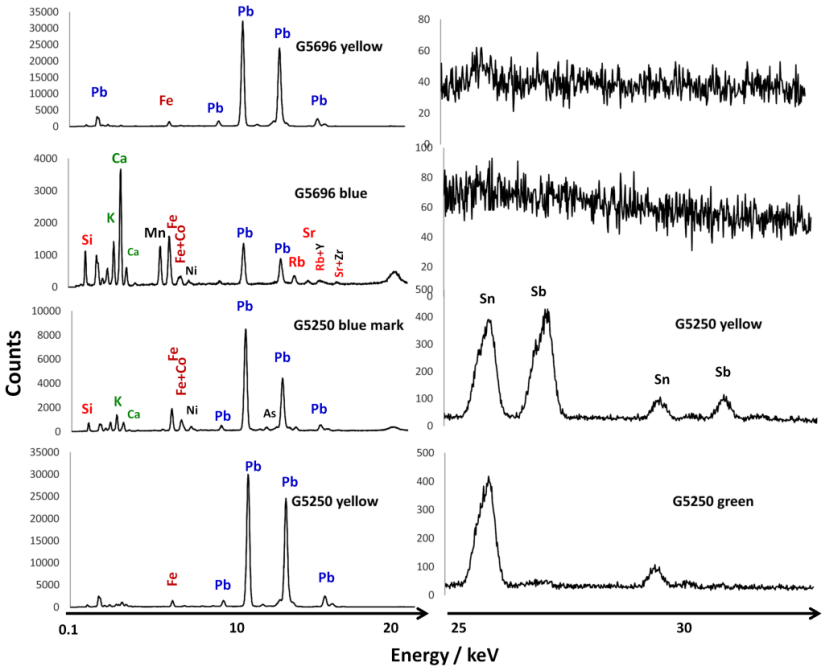

Figure 2. Representative XRF spectra of enameled porcelain (see Table 1 for details)

Figure 4 presents the spectra of metalware R958 and R975 for different colors. Here tin is detected in all colors due to the need for opacification imposed by the metal substrate. The red color is obtained by gold nanoparticles (see the small peaks around 10-13 keV on either side of the intense lead peaks), in agreement with the Raman analysis [39]. Generally the gold signal is difficult to see for the pinks and reds obtained by the gold nanoparticles, as for example for the pink of the R1175 porcelain (Figure 4). On the other

hand, the gold signature is intense for the golden areas (R1175) and as usual silver is detected, the silver improving the gold-ceramic bond [89,97]. The black color is obtained with a mixture of manganese and copper oxides as usual, that is consistent with the spinel Raman signature [23,26,29,98].

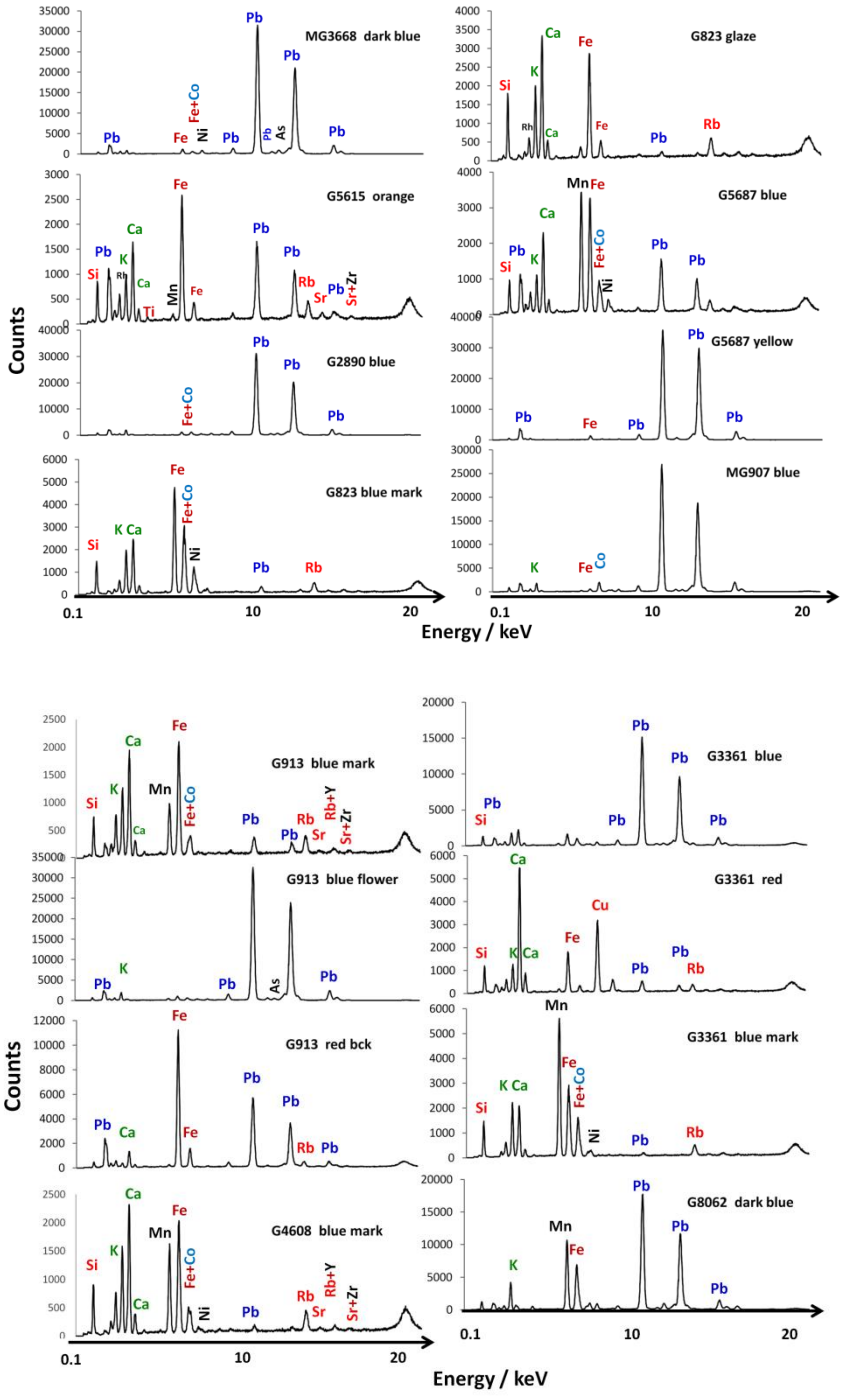

Figure 3. Representative XRF spectra of enameled porcelain (see Table 1 for details)

Table 2 summarizes the conclusions that can thus be drawn from the 'simple' visual examination of the spectra.

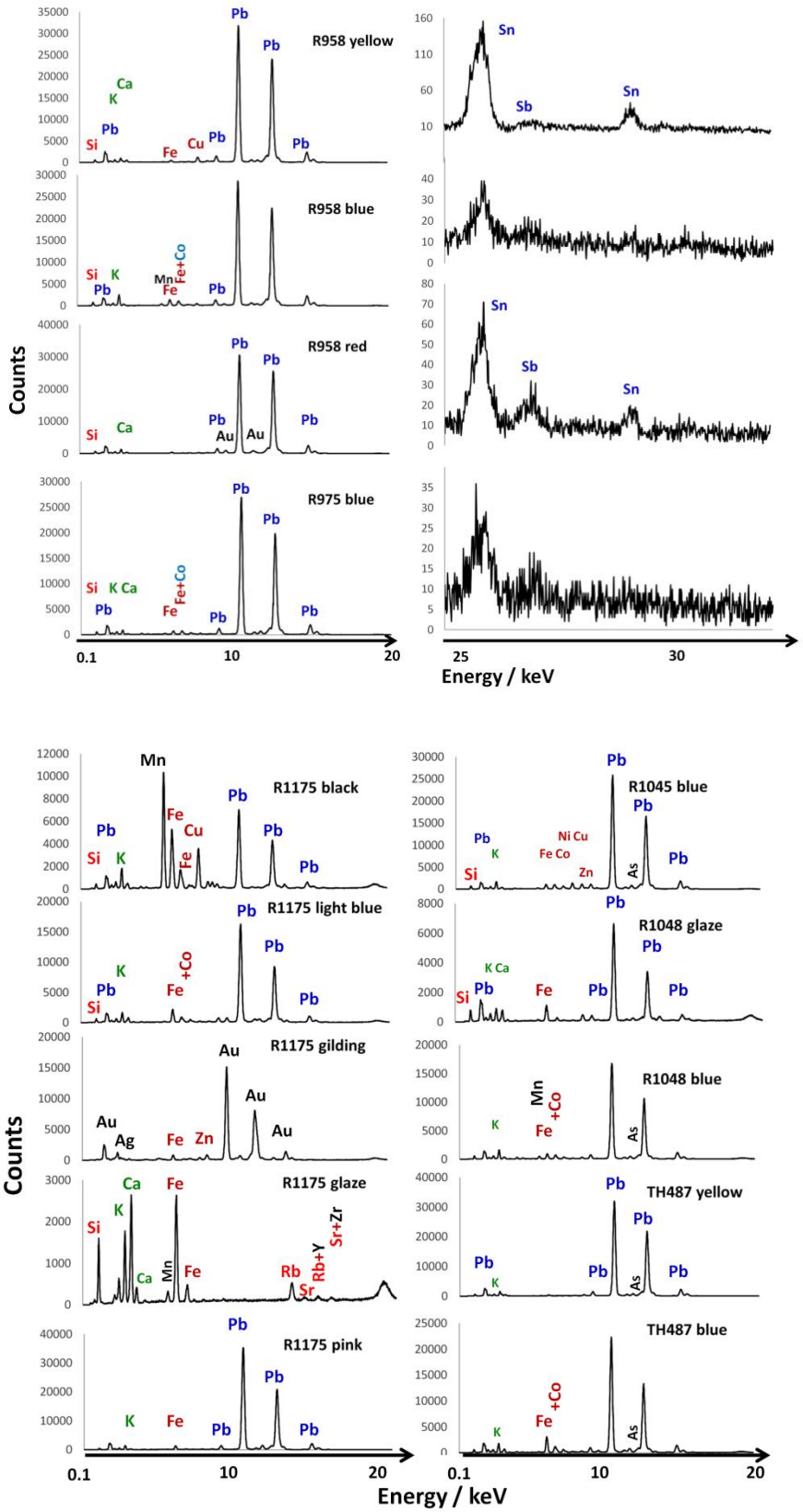

Figure 4. Representative XRF spectra of enameled porcelain and metalware (see Table 1 for details)

The other visually detectable elements are fluxes (potassium and calcium) and their associated impurities (rubidium and strontium); raw material impurities such as yttrium, zirconium and uranium, other coloring transition metals such as copper, manganese already mentioned, and those associated either with iron (titanium), or with nickel, zinc, etc. and arsenic are also obvious. [33] The main peak of arsenic (Kα) is superimposed for the resolution of pXRF instruments with the main peak of lead (Lα) and therefore only the second peak (Kβ) is observable, a little before the second peak of lead.[15,18] Figure 4 shows many examples. Iron presents a doublet with an intense Kα peak with a small Kβ peak attached, about 5 to 6 times weaker.[15,18] This last peak is for the resolution of pXRF instruments almost confused with the Kα peak of cobalt. Assessing the intensity and width of the peak helps to visually identify the amount of cobalt. To go further in composition comparisons, precise signal processing is necessary.

Table 2. Comparison between main coloring elements and associated ones, fluxing elements and phases identified y Raman microspectroscopy.

Inventory Number (expected date of production)	Color	Coloring elements and associated elements (*minor*)	Flux (major, medium, *minor*)	Raman identified phase [38,39,43]	Remarks
R1041 (1722-35)	glaze	Fe	Ca,K	-	
	blue	Co,Fe,Ni,As	Pb,*K*	-	European Co
	yellow	Fe,Zn,Sn	Pb,*K*	-	
	pink/rose bck	Zn,Au	Pb,*K*	-	Au° NPs
R1175 (1735)	glaze	Fe,Mn	Ca,K	Glassy	
	black	Mn,Fe,Cu,Co	K,Pb	spinel	
	light blue	Fe,Co	Pb,K	-	
	blue	Fe,Co,Ni,As,Cu,Zn	Pb,K	As-apatite	European Co
	pink	Fe,As,Zn	Pb,K	NPs	Au° NPs expected
	gilding	Au,Ag,Zn	Pb	-	
	white	As,Zn,Fe	Pb,K	-	
R1177 (1735)	glaze	Fe,	K,Ca	glassy	
	pink/rose	Zn,As,Fe	Pb,K	NPs	Au° NPs expected
	yellow+*black*	Zn,Sn (Mn,Fe)	Pb,K	Lead-tin yellow	
R1045 (1730-45)	glaze	Fe	K,Ca,*Pb*	Glassy	
	blue bck	Co,Fe,Ni,Cu,Zn,As	Pb,*K*	As phase	European Co
TH487 (1730-35)	blue	Fe,Co,As,Ni	Pb,*K*	As phase	European Co
	yellow	Sn,Zn,As	Pb,*K*	Glassy+lead-tin yell tr.	
	orange	Sn,Zn,As,Fe	Pb,*K*	NPs	Au°/Cu° NPs?
	red/rose	Zn,Fe,As	Pb,*K*	-	
	black	Fe,Mn	K,Pb	-	
R1048 (1740-60)	glaze	Fe	Ca,K	Glassy	
	blue	Mn,Fe,*Co*,Ni,Zn,As	Pb,*K*	As-apatite	Eur/Asian Co mixed?

	gilding (no gloss)	Au,Fe,Ag,Zn,Cu	K,Ca	-	
	gilding (glossy)	Fe,Au	K,Ca,*Pb*	-	
	yellow	Mn,Sn	Pb,*K*,*Ca*	Lead-tin yellow	
	red	**Fe**	Pb,*K*,Ca	Hematite + ?	
R958 (1730-96) (metal)	blue	Fe,Co,Cu,As,Mn	Pb,*K*	As-apatite	Asian+European Co
	yellow	Cu,As,Zn,Sn	Pb,*K*	As-apatite +lead-tin yell.	
	red/pink	Au	Pb,K	-	Au° NPs
	rose/pink	As,Sn	Pb,K	As-apatite	Au° NPs expected
	yellow-green	As,Cu,Sn	Pb,K	As-apatite+lead-tin yell.	
	green	Cu,As	Pb,K	As-apatite	
	gilding	Au,Sn,(Sb)	Pb,K	-	
	turquoise bck	Cu,As,Fe,(Sn)	Pb,K,*Ca*	-	
R975 (1730-96) (metal)	blue	Co,Fe,As,Ni,(Sn)	Pb,*K*	As-apatite	European Co
	yellow	Zn,Sn,(As)	Pb,*K*	As-apatite +lead-tin yellow	
	white	As,Fe,(Ni,Cu)	Pb,K	As-apatite	
	green	Cu,Zn,As,(Sn)	Pb,*K*	As-apatite	
	light green	Cu,Zn,Sn,As	Pb,*K*	As-apatite	
	pink/rose	Fe,As	Pb,*K*	As-apatite	Au° NPs ?
	black	Mn,Fe,Cu	Pb,*K*		
G5687 (midd 17th c.)	blue	Mn,Fe,(*Co*)	Ca,K,*(Pb)*	glassy	Asian Co
	yellow	Fe	Pb	glassy	
	red	Fe	Pb,*Ca*	hematite	
	green	Cu	Pb	glassy	
	black	Cu,*Mn*,*Fe*	Pb	spinel	
	paste	Fe	Ca,*K*,*(Pb)*	-	
G5696 (1700)	glaze	Fe	Ca,*K*	-	
	blue	Mn,Fe,(Co)	Ca,K,*Pb*	-	Asian Co
	blue mark	Mn,Fe,(Co)	Ca,*K*	-	Asian Co
	yellow	Fe	Pb	-	
	green	Cu	Pb	-	
	red	Fe,(Cu)	Pb,Ca	-	Cu° NPs ? or hematite
	paste	Fe	K,*Ca*	-	
G3361 (1700)	glaze	Fe	Ca,*K*	-	
	blue	Fe,Co,*Cu*,*As*	Pb,*Ca*,*K*	As-apatite	European Co
	blue mark	Mn,Fe,Co	K,Ca	-	Asian Co,underglaze
	red	Cu,*Fe*	Ca,*K*	quartz	Cu° NPs ?
	rose/mauve	Fe,Co,Cu,As	Pb,*K*,*Ca*	As-apatite	Cu° or Au° NPs?
	green	Cu	Pb	glassy	
	yellow-green	Cu,Sn	Pb	Lead-tin yellow	
	white	Fe,Cu,As	Pb,*Ca*	As-apatite	
G5250 (1715-22)	glaze	Fe	K,Ca	-	
	blue mark	Fe,Co,*Ni*,As	Pb,*K*,*Ca*	-	European Co overglaze

	dark blue	Co,As,Ni	Pb,*K*	As phase	Co peak too strong?
	yellow	Fe,*Sn,Sb,Zn*	Pb,*Ca*	Sb pyrochlore	
	green	Sn,Cu	Pb,*K*	-	
	yellow-green	Cu,Fe,Sn	Pb	Lead-tin yellow	
	rose/mauve	Fe,As,*Au*	Pb, *K,Ca*	NPs signature	Au° NPs
	black	Fe	Pb,*Ca*	-	
	white	As,Fe	Pb,*K*	-	
G913 (1723-35)	glaze	Fe	Ca,K	-	
	blue mark	Fe,Mn,(*Co*)	Ca,K	-	Asian Co underglaze
	blue flower	Fe,Co,Mn,*Ni,Cu,As*	Pb,K	-	Eur/Asian Co mixed ?
	red background	Fe	Ca,*Pb*	Hematite	
	white	Fe,*Mn,As,Co*	Pb,*K*	-	
	yellow	Fe	Pb	Glassy+lead-tin yell. Tr.	
	green	Cu,(*Sn,Sb)*	Pb	Glassy	
	black	*Mn,Fe,Ni,Cu*	Pb	Spinel	
	paste	Fe	K,Ca(*Pb*)	-	
G4806 (1723-35)	glaze	Fe	Ca,K	-	
	blue mark	Mn,Fe,(*Co)*	Ca,K	-	Asian Co underglaze
	blue	Fe,(*Co,Cu,As*)	Pb,*K*	Glassy	European Co
	yellow	Fe	Pb	Glassy+lead-tin yell. tr.?	
	green	Cu	Pb	-	
	white	*Fe*	Pb	hematite	
	rose	*Mn,Fe*	Pb		+Au° NPs ?
MG3668 (2nd half 18th c.)	dark blue	Fe,Ni,Co,As	Pb,*K*	As-apatite	European Co
	yellow	Fe,Sn	Pb,*Ca*	Lead-tin yellow	
	rose/pink	As,Fe,Zn	Pb	NPs	Au° NPs
	white	As,Fe	Pb	-	
	black	Cu	Pb	Spinel	
	turquoise	Cu,As,*Sn,Fe*	Pb	-	
	yellow-green	Cu,Sn,As,*Fe*	Pb	As-apatite+lead-tin yell.	
G823 (18th c.)	glaze	Fe	Ca,K	-	
	blue mark	Mn,Fe,(*Co*)	Ca,K	-	Asian Co underglaze
	dark red	Fe	Pb,*Ca*	hematite	
	orange	Fe	Ca,*Pb,K*	hematite	
	dark green	Cu	Pb	glassy	
MG8062 (19th c. ?)	dark blue	Fe,Co,As,(*Cu)*	Pb,*K*	As phase	Eur. Co : <1850!
	light blue	Fe,Co,As	Pb,*K*	As-apatite	Eur. Co : <1850!
	brown bck	Fe,*Ti*	K	-	
G5615 (19th c.)	glaze	Fe	Ca,K,*Pb*	-	
	green	Cu	Pb	-	
	orange	Fe	Ca,K,*Pb*	-	
	yellow	Fe,Sn,*Cu*	Pb	-	

	black	Cu,Mn,Fe	Pb	-		
G4939 (19th c.)	glaze	Fe	K,Ca	-		
	rose bck	Fe,**Au**,Zn	Pb,*K*	-		Au° NPs
	blue mark	Mn,Fe,*Co*	K,Ca	-		Asian Co underglaze
MG907 (19th c.)	blue	Co,*As*	Pb,*K*	-		Co purity >1850
	dark blue	Co,*Fe,Cu,As,Ni*	Pb,*K*	-		Co purity >1850
	blue mark	Fe,Mn,(*Co*)	Ca,K	-		Asian Co underglaze
	white	*As,Cu,Fe,Sn*	Pb	-		
	yellow	Sn,*Fe,Cu*	Pb	-		
	green	Cu,*Co,Fe,As,Sn*	Pb,*K*	-		
	gilding	Au,*Ag,Fe,Cu*	*K,Ca*	-		
	red	Fe	Ca,K,*Pb*	-		
	paste	Fe	K,*Ca*	-		
G2789 (19th c.)	glaze	Fe	K,Ca	-		
	red mark	Fe	K	-		
	black	Cu	Pb	-		
	green	Cu	Pb	-		
	light green	Cu,Sn,*As,Fe*	Pb	-		
	white	As,Cu,Fe	Pb	-		
	'gilding'	Cu	Pb	-		False gilding
	gilding	Cu,*Fe,Au*	Pb,*K,Ca*	-		True Au° gilding
	paste	Fe	K	-		
G2890 (19th c. ?)	blue	Fe,Co,Cu,*Ni,Zn,*As	Pb,*K*	-		Eur. Co >before 19th c.
	dark mark	Fe	K,Ca	-		
	yellow	Sn,Fe,Zn	Pb,*K*	-		
	rose	Fe,Sn,*Au,Zn,Cu*	Pb,*K*	-		Au° NPs
	green	Cu,Fe,Sn	Pb,*K*	-		
	orange	Mn,Fe,Sn	Pb,*K*	-		
	black	Mn,Fe,Cu	Pb,*K*	-		
	paste	Fe	K,Ca	-		

Eur. : European; tr.: traces; -: not studied; NPs: nanoparticles

As already observed in the study of the Baur Foundation bowls with imperial mark [36,37], the cobalt used for the underglazed marks is rich in Mn, which is in agreement with an application of the mark on the porcelain green paste in Jingdezhen kiln with a cobalt from Asian sites. On the contrary, the blue areas of the decorations use cobalt of complex composition (As, Ni, Cu) in accordance with an imported material and the enamel is lead-based. The *wucai* G5687 and G5696 pieces, the oldest in our selection, use Asian cobalt for the decor. As concluded from the Raman analysis, the G3361 pot appears to be one of the first objects using imported materials. G2890 bowl expected from 19th century is made with impure European cobalt that is consistent with a production before development of cobalt refining, i.e. before ~1850. False copper-based gilding in

combination of true Au° gilding is identified for G2780 bowl. Such technique was already identified in 18th century Meissen 'gilded' *boccaro* 'porcelain' [99].

For a clear identification of the use of Cu° or Au° NPs for red to violet/mauve color combination of Raman and XRF is required due to the low amount of metal NPs required and hence its difficulty to detect by XRF. Combination of a 'simple' Raman signature of the glassy coating with identification of Fe element attests the use of iron ions (Fe^{3+}) to obtain the yellow color (e.g. G4826, G5687 and G5696). Traces of lead-tin are detected by Raman microspectrometry (e.g. G913 and G4806).

3.2. Towards a semi-quantitative comparison

We underlined in the experimental part the problem of the variability of the depth probed by the X-ray photons according to their energy,[70] penetration depth being able to be very lower (light elements) or very higher (heavy elements) than the thickness of the layer of colored enamel.[100] Only for the transition metals the characteristic peaks are located in an energy range inducing a penetration of the same order of magnitude as the standard painted enamel layer (100-200µm).[38,41] In addition, by nature, a painted enamel decoration is heterogeneous in chromophore in the 3 directions of the colored layer and this for lower scales or of the order of magnitude of visual acuity (a few microns).[101] Unlike 'solid' glass objects (crockery, stained glass) or thick 'monochrome' enamel layers – a layer of celadon enamel can exceed several millimeters [19] – the concept of composition therefore makes no sense for painted enamels and we have proposed a particular procedure for comparing enameling techniques, the comparison of the localization of the characteristic signals of the different chemical elements (after correction of the continuous background as possible for example with the Artax data processing software) in ternary diagrams relevant to raw material composition and ceramic process.[36,37] Clustering data should correspond to rather similar element content in the analyzed volume.

3.3. Comparison of silicate matrices

An enamel is a totally amorphous glass, whether or not containing chromophore ions, bubbles or a formation of several amorphous phases, or else a glass-ceramic (i.e. a composite material containing a dispersion of phases, introduced before firing into the precursor powder (pigment containing one or more chromophores or opacifier characterized by a higher optical index than that of the silicate matrix; these phases must be very chemically stable so as not to be attacked, dissolved by the enamel in fusion during firing) or forming on cooling from the saturation of certain elements of the molten enamel. We will consider the elements having the role of flux, that is to say lowering the melting point, controlling the viscosity, etc.: potassium, calcium, lead and arsenic (the method cannot detect boron, lithium and sodium), these elements being able to have other specific effects on thermal expansion, chemical resistance, opacification, etc.[24-26,29] The natural impurities of these elements, namely rubidium, strontium will be also considered (Figure 5).

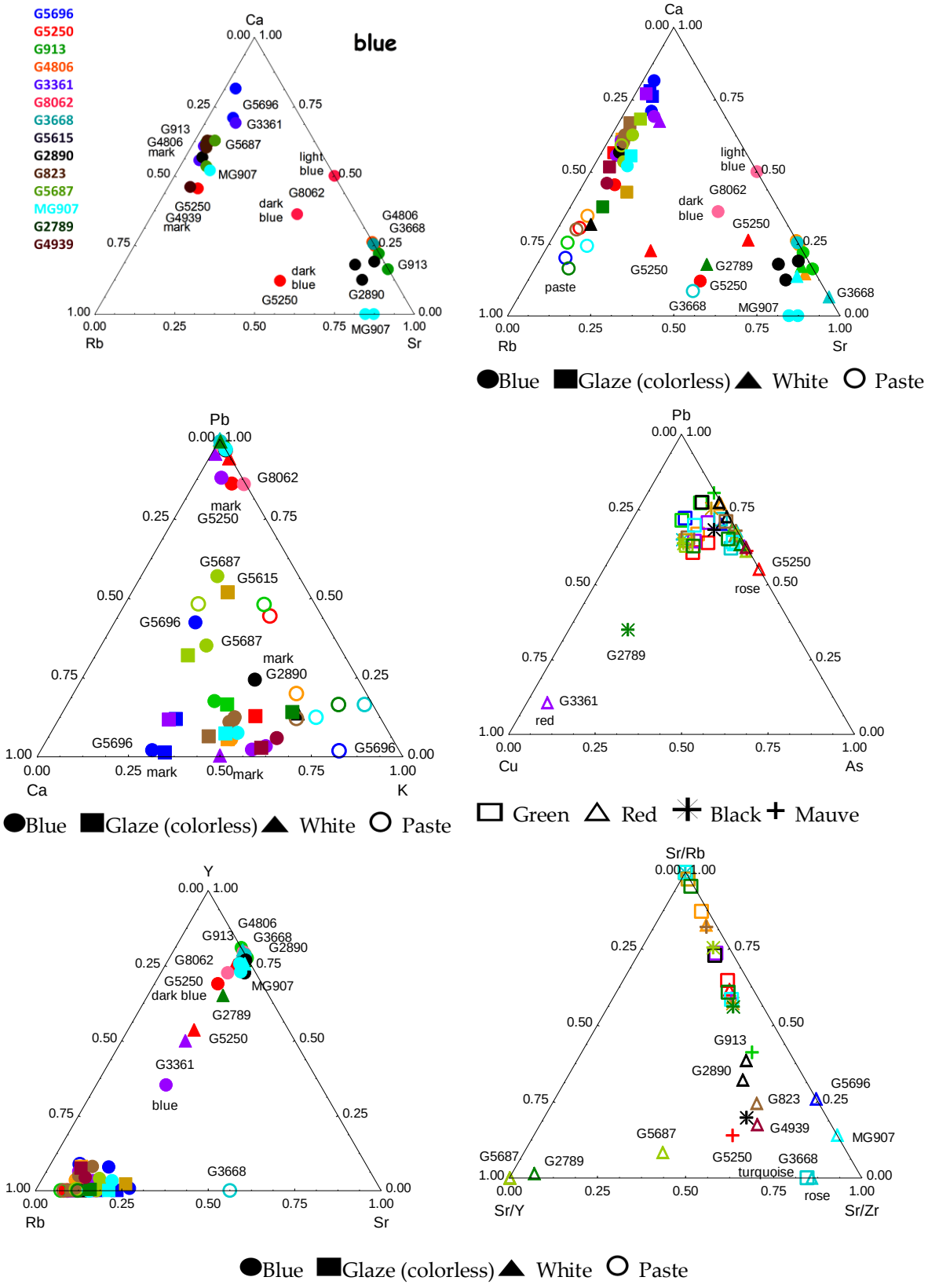

Figure 5. Comparison of flux elements (Pb, Ca, K) of matrices of blue, white or colorless, green, nouge/pink/mauve enamels and pastes and associated elements (Sr, R, Y) (Coll. mnaa-Guimet).

The Ca-Rb-Sr ternary (Figure 5) constructed from 'blue' enamels highlights 3 or 4 clusters: two large groups, one parallel to the Ca-Rb side and the other enriched in strontium; MG8062 (19th c.) forms an intermediate cluster like the *falangcai* bowl blue G5250. We therefore have 3 types (origins) of raw materials (which we will call RMCa, RMSr and RMInt). The same classification is possible for enamels of other colors. Paste is located in the RMCa cluster, which leads to associate this group with the use of raw materials from Jingdezhen. From the Ca-Rb-Sr ternary diagram it is clear that the white enamel of artifact G5250 is rather heterogeneous but rather similar to that of G8062 blue one. A third group or a mixture of the other two groups explains the location of the enamels of the Yixing bowl MG8062 and the *falangcai* bowl G5250. The Pb-Ca-K and Pb-Cu-As ternaries provide additional information.

We will first discuss the objects in Figure 2 (mnaa-Guimet Collection, Table 1). The first separates the enamels in which lead constitutes the main flux (all located towards the Pb top summit) from the enamels (and paste) whose surface has been polluted by the lead evaporating during the firing of the overglaze (PbO is very volatile in the above 850°C). Potassium-rich pastes (located on the Pb-K side) are also separated from most calcium-rich glazes. The Pb-Cu-As diagram highlights 3 special cases: the black background of bowl G2789 is rich in copper (well-established technique [23,26,29,98]); the pink/rose of the G5250 bowl is enriched with arsenic and as the Raman analysis indicates the use of metallic nanoparticles, coloring by gold nanoparticles is expected; the red color of the rose in the G3361 pot is obtained with Cu° nanoparticles (which is in agreement with the Raman analysis which indicates that the red color is not obtained as conventionally by hematite [38]). The use of copper nanoparticles (Cu°) is a techniques used since 10th century (Jun ware) by Chinese potters. [102-106]

The Y-Rb-Sr ternary classifies the enamels into two groups, a main group and a second on a line defining the same Y/Sr ratio where the pot G3361 and the bowl *falangcai* G5250, the bowl G2789, MG907 and MG3668 are located. The ternary constructed by normalizing the signal of strontium by the signals of rubidium, yttrium and zirconium highlights two aligned groups for defined Y/Zr ratios (colorless glazes are part of this group) and Rb/Zr. We find a relationship between certain enamels and glazes as for the pastes, which is consistent with the use of the same raw materials, those of Jingdezhen.

We find on the Pb-Ca-K diagram of Figure 6 the two groups of lead-based enamels and those unpolluted or little polluted during firing plus an intermediate group for the golden areas (R1175, R1045, R1048 and R1177 which would indicate a mixed matrix with an intermediate lead content and/or the addition of other fluxing agents. The same is true for the Pb-Cu-As diagram where this group is clearly identifiable. It is difficult to know if the distribution towards the Cu top is caused by the contribution of the metallic substrate for the artifacts R958 and R975 The two groups identified in Figure 6 for the Sr diagram normalized by Rb, Y and Zr are found and the alignment of the data showing the defined Y/Sr ratio is clear, the golden and white colors being richer in Rb while the

enamels of objects R1045, R1048, R1175, R1177 and TH487 (all Yongzheng period) are 'richer' in yttrium.

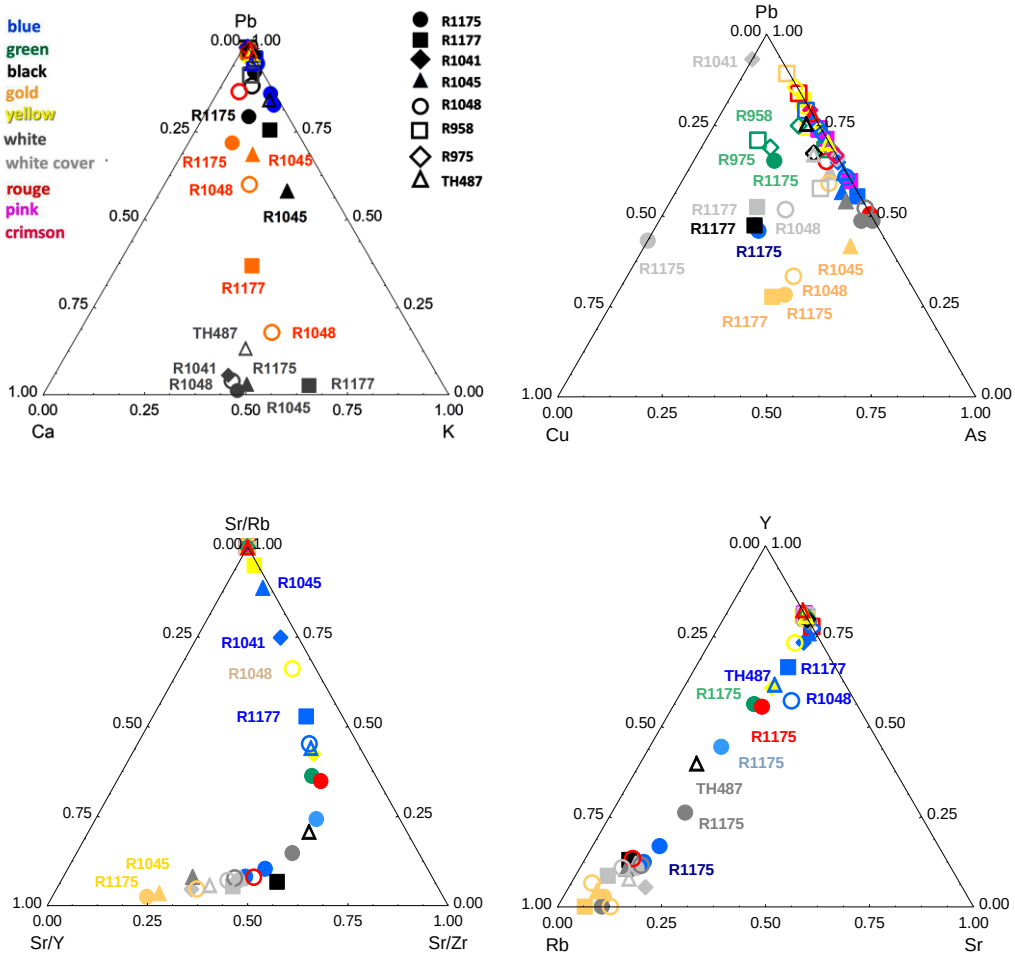

Figure 6. Comparison of flux elements (Pb, Ca, K) of enamel matrices and associated elements (Sr, R, Y, As) (Coll. Louvre).

3.4. Comparison of coloring agents

Figure 7 compares the distributions of the signals relating to the color blue, i.e. cobalt and the associated elements, arsenic, manganese and nickel. The source of cobalt in Europe is a potassium glass called smalt with about 10 to 20% wt CoO potassium.[33] Smalt was a by-product of the mining of silver, then of bismuth. Cobalt was specifically mined only at the end of 17th century. [33] Consequently the set of associated element depends both on the ore's composition and processing. Copper is either an addition to adjust the color or present in ancient cobalt sources (17th and before)[18,33]. On the Co-Pb-K diagram, two clusters can be distinguished, the series of blue marks (G3361, G4939, G5696, G4806, G823, MG907, G913) which correspond to underglaze marks, most of the potassium likely coming from the contribution of glaze above and around the blue lines, the analysis being carried out by the surface on a spot larger than blue line. The measurement for some having been made on different spots, the distribution of the points gives an illustration of the variability/error of the measurement. The mark of the

G5250 gives corresponds to lead overglaze enamel composition. The highest level of copper is observed for ancient objects, G5606, G3361 and G4806 as previously observed [18]. G2890 appears to be arsenic-free, consistent with production after 1850, as already noted with other criteria.

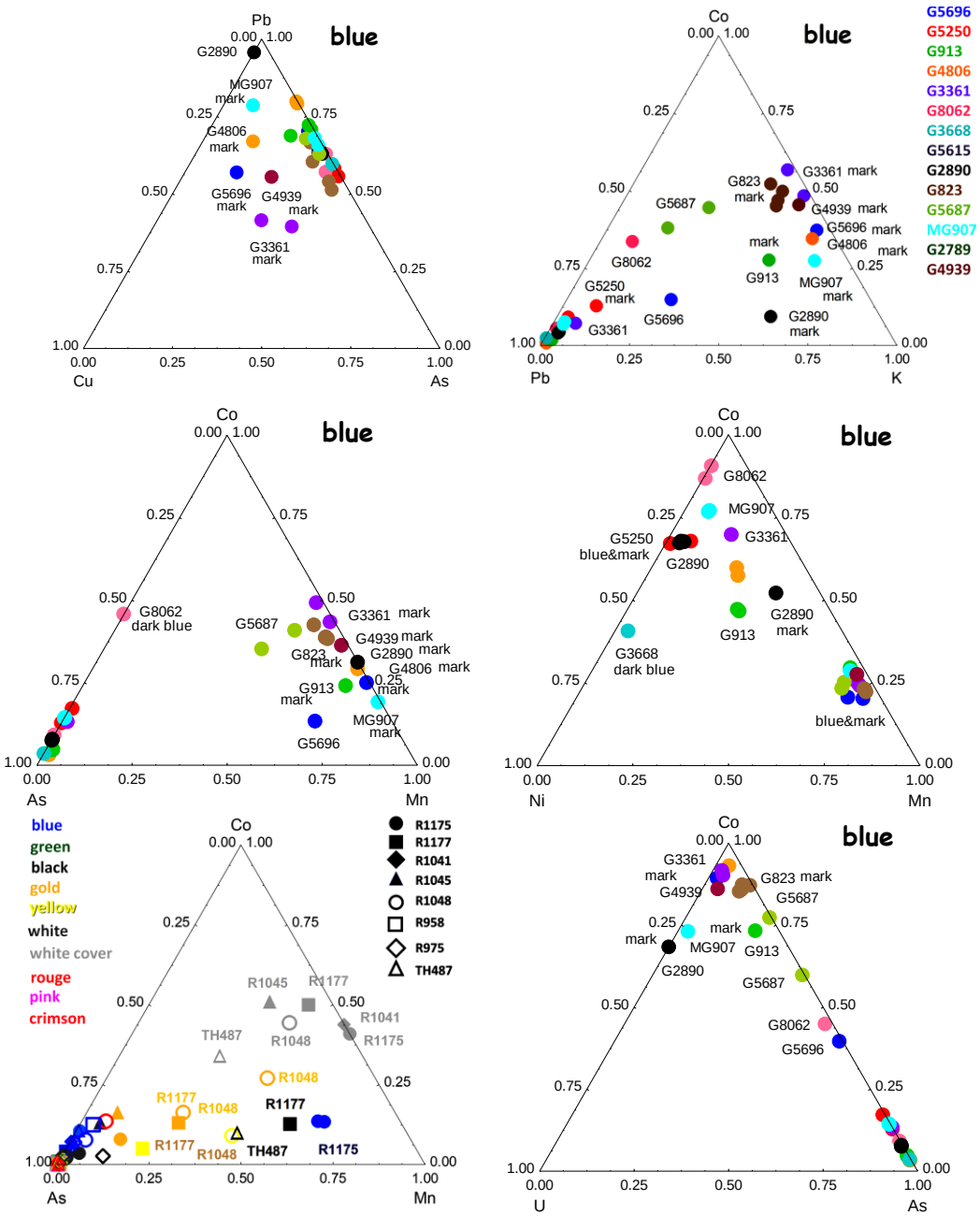

Figure 7. Comparison of elements associated with cobalt (Mn, Ni, U and As) for blue enamels (top and center, Coll. mnaa-Guimet) and for all enamels (bottom, Coll. musée du Louvre).

The Co-As-Mn diagram differentiates manganese-rich Asian 'cobalts' (marks of G3361, G4939, G4806, MG907, G823, and G913; patterns of G5687, G5696) from possibly arsenic-rich European 'cobalts' (patterns of G8062, MG907, G3361, G913, G4939, G4806).[33] The blue of the decor of the Yixing G3668 teapot is particular, which is con-

firmed by the Co-Ni-Mn diagram. This diagram specifies the differences between the different 'cobalts': the richest in manganese are G5687 (decor), G5696 (decor and mark), and marks for G823, G3361, G4806, G913, and MG907. We find that the bowl G8062 is made of 'pure' cobalt, so it production will be after 1850. For the artifacts of the Louvre museum (Figure 1), only the blue of R1175 is rich in manganese, all the other blues are rich in arsenic and can have thus been prepared with ingredients imported from Europe. Note the presence of arsenic in the red colored areas (R1045, R1048). Three hypotheses are possible: first, As-based opacifier has been dispersed in the red precursor powder or a background white layer has been deposited. Alternatively the arsenic can be associated to the red chromophore.

Figure 8 compares different diagrams relating to the colors yellow, orange, brown and gold. The Pb-Ca-K diagram highlights the colors where traces of lead are only pollution product when firing other colors: orange G823, orange G5615, golden MG907 and brown G8062; these cases are also distinguished by the presence of copper.

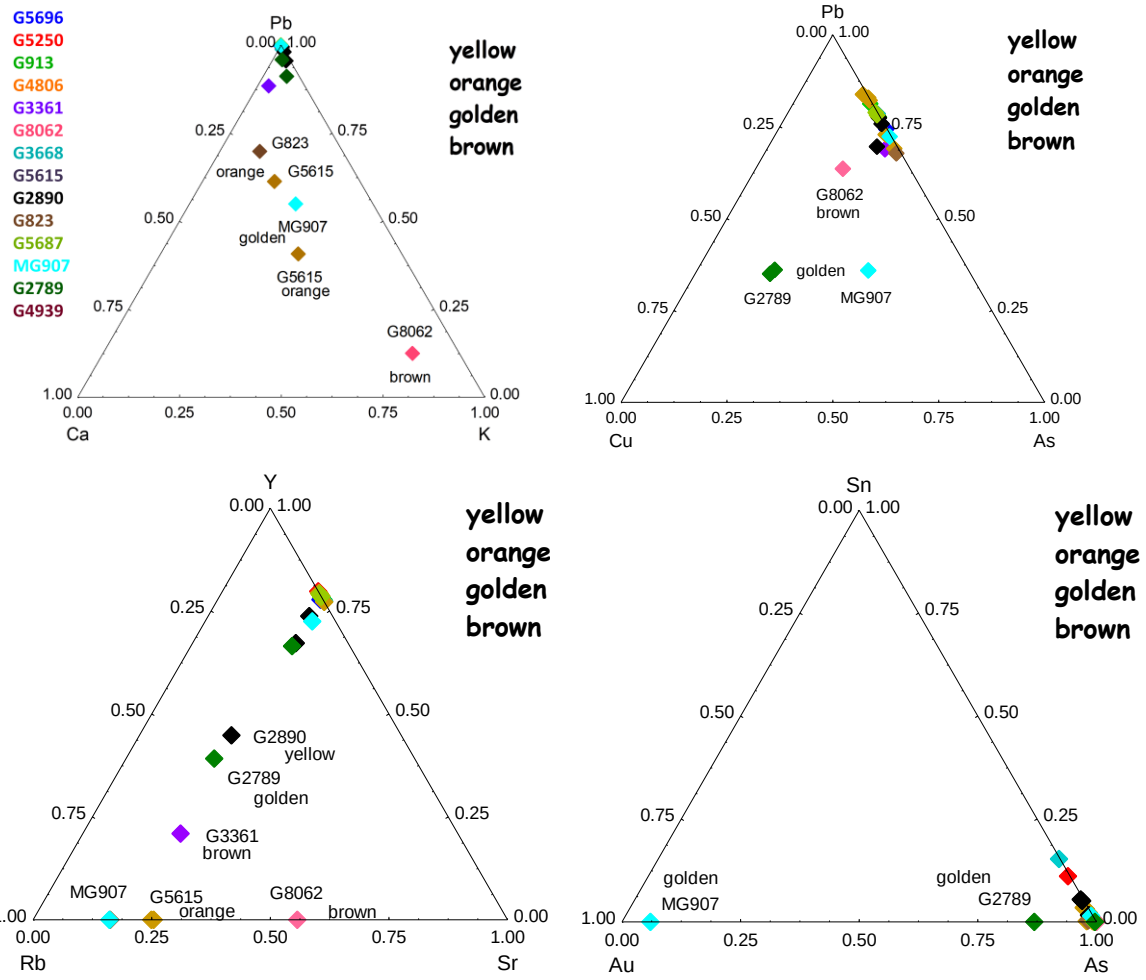

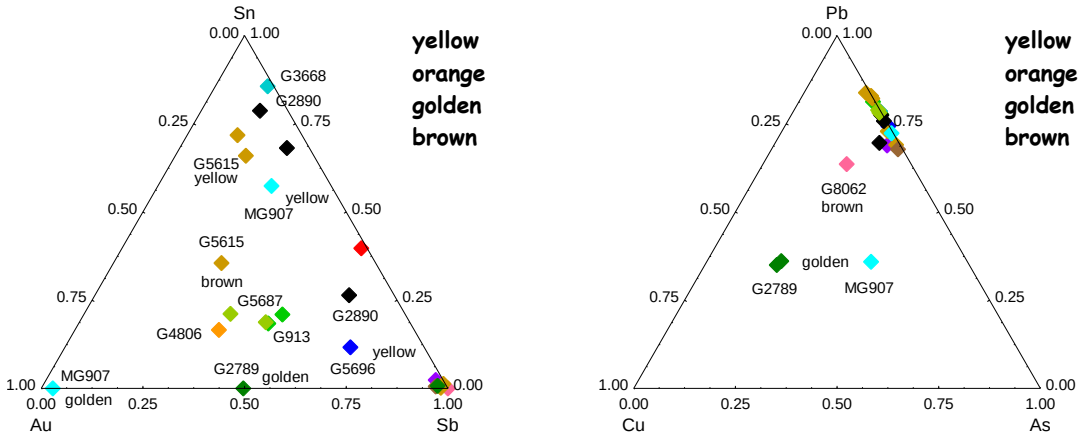

Figure 8. Comparison of elements associated with the colors yellow, orange, brown and gold.

Golden MG907 and MG2789 have different grades of gold, both containing some copper, with MG907 being the 'purest'. The Sn-Au-Sb diagram classifies these colors into three groups, tin yellows (G3668, G2890, G5615 and MG907); Naples yellow rich in antimony (G2789, G4806, G3361) and mixed Naples yellow (G5615, G5687, G913, G5615, G4806), different glazes can be observed on the same object.

3.5. Gold nanoparticle preparation

The comparison of the XRF signals relating to the elements Au, Sn and As for the different colors ranging from pink to violet and mauve, colors (Figure 9) that can be obtained by gold or copper nanoparticles but also by a red pigment such as hematite or hercynite will allow us to know the method of preparation of colloidal gold. Indeed it is established that in the 17th century in Europe two techniques were used for the preparation of colloidal gold from a solution of gold in *aqua regia* (mixture of nitric and hydrochloric acid): precipitation by addition tin (technique known as Kunckel or Cassius' purple)[107,108] or by adding arsenic (technique known as Perrot' or ruby glass)[109,110], these two techniques originating in Italy. By oxidizing, both tin and arsenic having several oxidation states lead to the reduction of gold ions into metallic nanoparticles. The colloidal gold signal is always very weak because the very high coloring power of the plasmon of the NPs means that a very small quantity is sufficient. Also zooms were made near the arsenic pole. We note that only the reds of metalware R958 and (Meissen imitating) porcelain R1048 contain a little tin, and almost no gold (red is obtained with iron oxide hematite, Table 2) for all the others tin is only traces (Figure 9, left). The maximum zoom (Figure 9, right) shows 2 groups, those where gold is associated with traces of tin (G2890 bowl, pink; G3361 pot, red; G4939 bowl, pink background) and all the others rich in arsenic. Only the colors of the first group can be considered Cassius purple. For the others, two solutions are possible: preparation by the Perrot method and/or voluntary addition of arsenic as an opacifier. Opacifier is likely for rose, or carmin not for red. So for G5687 17th c. wucai, G5696 17th wucai, G913 Yongzheng bowl, TH487 Yongzheng plate, G823 Qianlong plate, G2789 19th c. bowl, red MG907 bowl 19th c., and R958 Qianlong metal plate the Perrot' technique is the most likely.

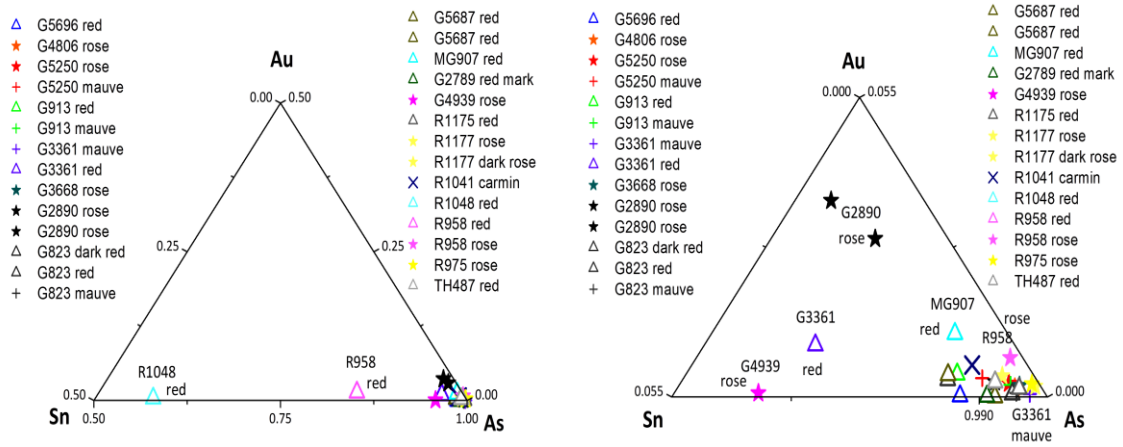

Figure 9. Comparison of elements associated with the use of gold.

4. Discussion: Comparison between Qing productions and with Ming ones

The objective of this work was to identify in a non-invasive way on the site of conservation of the pieces those whose glazes prepared by recipes or ingredients imported from Europe, as specified in the documents of imperial archives or in the correspondence of Jesuit missionaries.[3-5,11,13,14] The geological contexts of the regions where Chinese potters sourced their supplies during the Yuan, Ming and early Qing Dynasties, regions marked by the 'recent' Himalayan geological context differing greatly from that of European sources associated with old (Hercynian) massifs and therefore the elements associated with cobalt are very different.[33] This is why we will compare with the XRF signals the elements Mn and Fe ('Chinese' context) and Ni and As (European context), as already carried out with objects from the collections of the museums of L'Ariana and the Baur Foundation [36,37] for which we have also shown that major elements and impurities associated with materials Early eras of preparation of the silicate matrix (potassium, calcium, rubidium, strontium and yttrium) effectively classified the Chinese or European origins of the productions. The diagrams are shown in Figure 10. As in essence a painted decoration is built by varying the cobalt concentration, the XRF characteristic signals of the different elements are normalized with respect to the cobalt signal. Similarly, to compare the impurities of other raw materials, we normalize with respect to the silicon signal, which makes it possible to take into account the variable thickness of the enamel. This last normalization is coarser.

4.1. Enamelling technology

The Pb-K-Ca diagram normalized by the Si signal and the Y-Rb-Sr diagram visualize the high temperature underglaze decorations concentrated towards the Ca/Si apex (Ming & Yuan) and the lead-rich enamels towards the apex P/Si (essential Qing enamels).

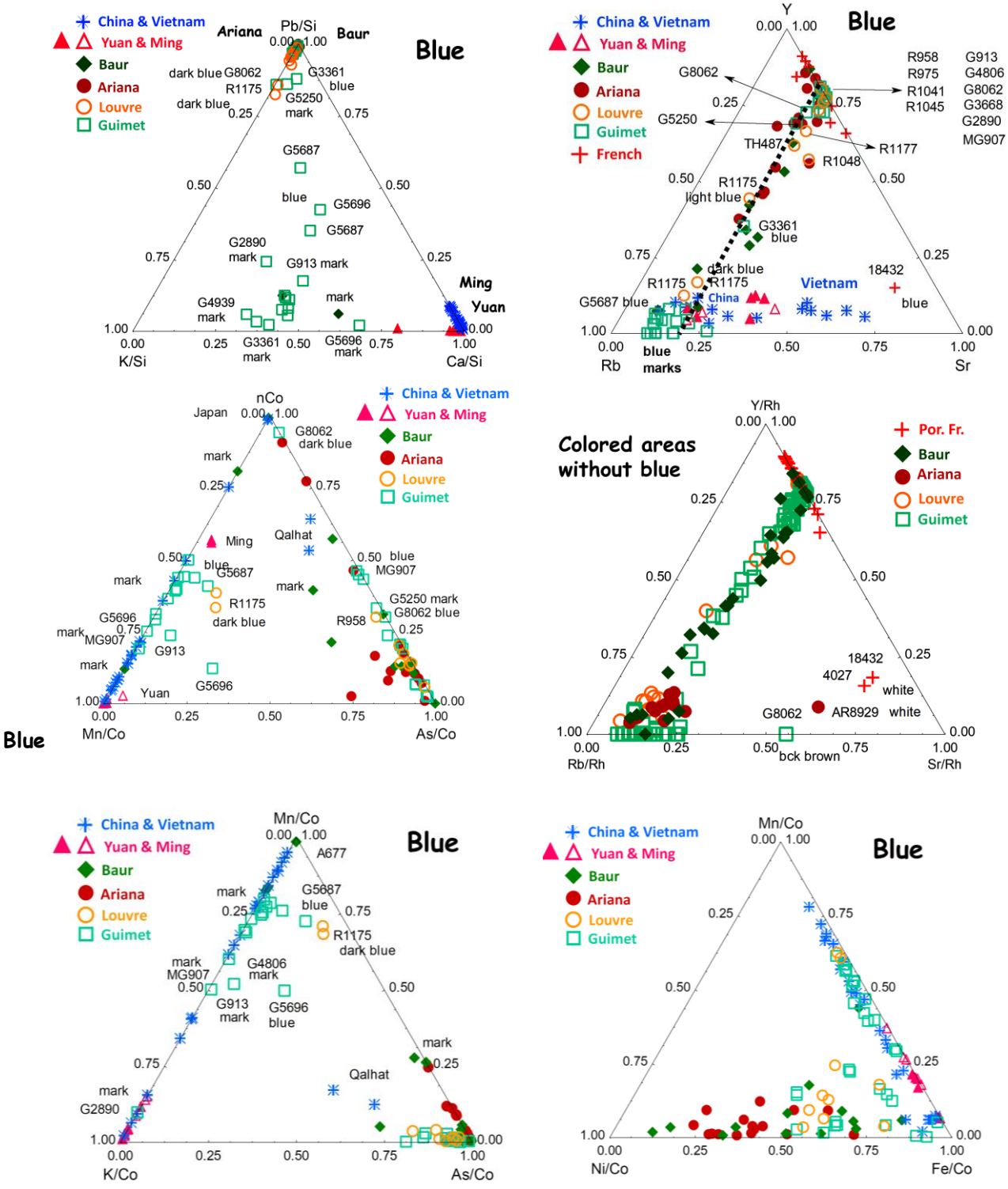

Figure 10. Comparison of elements associated with the blue colored areas for artifacts from different origins: Yuan and Ming Dynasty Private Musum Collection [44,45], archaeological shards issued from sites from Ming Dynasty period [46], Baur Fondation Collection [36,37], Ariana Museum Collection [36,37], French porcelain [18] and present study (Louvre and mnaa-Guimet museum Colections). Comparison is made with other colored areas.

Added to this are a number of enamels of objects from the mnaa-Guimet, roughly aligned for a K/Ca ratio; this indicates glazes with mixed Pb-Ca-K fluxes or glazes of variable thickness, the measurement of lead being made on a high thickness or the effect of the pollution of the surface of the glazes during the firing of the overglaze; this is why all the underglaze markings appear in the lower part. We find a similar configuration for the Y-Rb-Sr diagram. On this diagram we have also plotted the data for French soft-paste porcelain decorations [18]. The Y-Rb-Sr diagram shows three groups, i) enamels/glazes prepared with Chinese raw materials, rich in rubidium (Vietnam productions are enriched in strontium); ii) those prepared with European raw materials, rich in yttrium and iii) the intermediate cases explained by the use of a mixture of raw materials. We find the same distributions as for the pieces from the Ariana and Baur Foundation collections.[36,37] The differences between porcelain of Chinese/Vietnamese (Ming period) and French origins are obvious and Qing productions are aligned between these extremes, proving the mixture of 'Chinese' and imported ingredients. The list of objects in the decor using mainly European ingredients is listed in the figure. The more the value moves along the line parallel to the Y-Rb side, the more the proportion of Chinese raw materials increases; thus for underglaze marks we find belonging to the 'Ming' cluster. The results are similar for the other colors but with more intermediate data, probably due to the varying proportions of opacifier according to the colors

The nCo (normalyzed by Rh counts)-Mn/Co-As-Co diagram classifies objects made with 'pure' cobalt from the chemical industry (a 20th c. Japanese porcelain and the bowl MG8062 (19th c.) and the mark reported later from a bowl in the Baur Fondation Collection (#616)[36,37] This also classifies cobalt associated with arsenic and those rich in manganese, i.e. made with 'cobalt' of Chinese traditions. In the latter there are the marks affixed at Jingdezhen underglaze. Intermediate data indicate the use of a third type of cobalt (e.g. G5687 and G5696 wucai) or mixture (R1175). The classification of blue decorations is done with the Mn/Co-K/Co-As/Co and Mn/Co-Ni/Co-Fe/Co diagrams. We find the differences between the cobalt of the underglaze brands and that of the overglaze enamels. The comparison with the measurements on the objects of the L'Ariana museum, attributed to the workshops of Canton shows that the cobalt used in the latter is richer in nickel, therefore a European source of this type [33]. We also find that objects from the mnaa-Guimet use 'Chinese' cobalt and mixtures.

Figure 10 compares the signal of the main elements present in the areas colored in yellow, green/turquoise, and brown/orange. The data has been normalized with the source signal to improve the comparison. We see that the orange color is a color of glaze and not lead enamel. The Zn-Sn-Sb and Co-Cu-Sn ternary diagrams show that the green/turquoise colors are always colored by Cu^{2+} but varying levels of zinc are present, presumably due to varying origins of copper. The variability of solid pyrochlore solutions with very different proportions of Sn and Sb is also evident, 'pure' tin yellow being rare.

5. Conclusions

The study demonstrates the potential of on-site and completely non-invasive analysis to compare enameling technologies. The complementariness of pXRF and mobile Raman μspectrometry is obvious. Although the analysis is made by the surface on a heterogeneous material, the procedure of visualization of the results makes it possible to classify the enamels according to the elementary ratios and therefore to the raw materials. High efficiency is noted for the blue (and green) color due to the different geological contexts of the cobalt sources in Asia and Europe – more work on the characterization of cobalt ores are needed to go further -, for the yellow and green colors due to the complex non-stoichiometry of the pyrochlore pigment (tin yellow-Naples yellow).

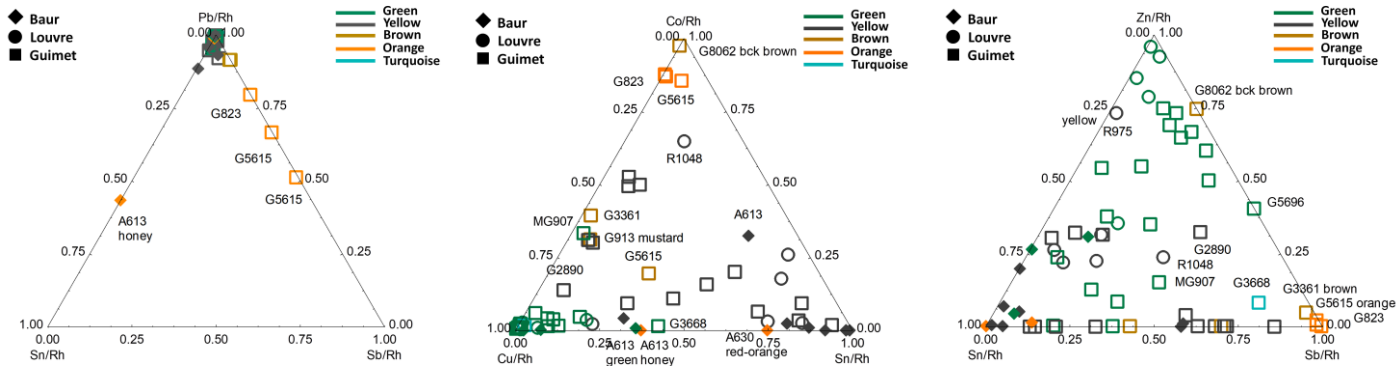

Figure 10. Comparison of signal of elements associated with the yellow, green/turquoise, and brown/orange colored areas (normalized with Rh signal).

The procedure is also efficient in distinguishing between the different nanoparticles used to prepare from rose to violet color. The comparison of the elements present in marks is also very instructive to detect posterior addition. Unfortunately the molecular techniques used here cannot identify the use of borax (possible by PIGE or by Raman under blue laser excitation) nor fluxes such as sodium (measured by SEM-EDS, PIXE and PIGE) and lithium (PIGE)[57]. The comparison of XRF signal levels relative to yttrium, rubidium and strontium signals is particularly effective in identifying the use of European raw materials. The cobalt-manganese-nickel and cobalt-manganese-arsenic diagrams identify the different sources of cobalt and help date the period of production. The combined Raman -pXRF procedure makes it possible to assess for each color of each artefact the degree of use of local raw materials and those imported

Supplementary Materials: The following supporting information can be downloaded at:www.mdpi.com/xxx/s1, Figure S1: title; Table S1: title; Video S1: title. XRF data ??

Author Contributions: Conceptualization, P.C.; methodology, P.C. and G.S.F.; investigation, X.G., J. B., and P.C..; resources, B.Z. C.D. and J.-B.C.; writing—original draft preparation, P.C., and G.S.F.; writing—review and editing, P.C., G.S.F., J.B., B.Z., C.D. and J.-B.. All authors have read and agreed to the published version of the manuscript.

Funding: The research in France was partialy funded by the French Agence Nationale de la Recherche ANR EnamelFC project—19-CE27–0019-02.

Data Availability Statement: Not applicable.

Institutional Review Board Statement: Not applicable.

Informed Consent Statement: Not applicable.

Acknowledgments: Museum direction and staff are cordially thanked for their support and their authorization to study the artifacts. Ludovic Bellot-Gurlet (Monaris, Paris) and Pauline d'Abrigeon (Baur Fondation, Musée d'arts d'Extrême-Orient, Genève) are kindly acknowledged for many discussions as well as Mathieu Lebon (MNHN) for the availability of XRF instrument.

Conflicts of Interest: The authors declare no conflict of interest.

References

1. Montanari, R.; Murakami, N.; Alberghina, M.F.; Pelosi, C.; Schiavone, S. The Origin of overglaze-blue enameling in Japan: New discoveries and a reassessment. *J. Cult. Herit.* **2019**, *37*, 94–102.
2. Landry-Deron, I. Les Mathématiciens envoyés en Chine par Louis XIV en 1685. In *Archive for History of Exact Sciences*; Springer: Berlin/Heidelberg, Germany, 2001; pp. 423–463. ⟨halshs-00676823⟩
3. Loehr, G. Missionary-artists at the Manchu Court. *Trans. Orient. Ceram. Soc.* **1963**, *34*, 51–67. Available online: https://www.orientalceramicsociety.org.uk/publications/transactions/4 (accessed on 2 June 2022).
4. Shih, C.-F. Evidence of East-West exchange in the eighteenth century: The establishment of painted enamel art at the Qing Court in the reign of Emperor Kangxi. *Natl. Palace Mus. Res. Q.* **2007**, *24*, 45–94.
5. Xu, X.D. Europe-China-Europe: The Transmission of the Craft of Painted Enamel in the Seventeenth and Eighteenth Centuries. In *Goods from the East, 1600–1800 Trading Eurasia*; Berg, M**.,** Gottmann**, F.,** Hodacs**, H.,** Nierstrasz**,** C., Eds.; Palgrave Macmillan: London, UK, 2015; pp. 92–106.
6. Palace Museum. *Treasures from Oversea Countries, Exhibition Catalogue of Kulangsu Gallery of Foreign Artefacts from the Palace Museum Collection*; Gugong Chubanshe: Beijing, China, 2011.
7. Kleutghen, K. Chinese Occidenterie: The Diversity of "Western" Objects in Eighteenth-Century China. *Eighteenth-Century Stud.* **2014**, *47*, 117–135.
8. de Rochebrunne, M.L. Les porcelaines de Sèvres envoyées en guise de cadeaux diplomatiques à l'empereur de Chine par les souverains français dans la seconde moitié du XVIIIe siècle. In *Des Arts Diplomatiques. Les Cadeaux Diplomatiques Entre la Chine et l'Europe aux XVIIe-XVIIIe Siècles. Pratiques et Enjeux*; Zhao, B., Landry-Deron, I., Simon, F., Eds.; *Extrême-Orient Extrême-Occident* **2019**, *43*, 81–92.
9. Finlay, J. Henri Bertin and Louis XV's Gifts to the Qianlong Emperor. In *Des arts diplomatiques. Les cadeaux diplomatiques entre la Chine et l'Europe aux XVIIe-XVIIIe siècles. Pratiques et enjeux*, Zhao, B., Landry-Deron, I., Simon, F., Eds, *Extrême-Orient Extrême-Occident*, **2019**, *43*, 93–112.
10. Guo, F. Presents and Tribute: Exploration of the Presents Given to the Qianlong Emperor by the British Macartney Embassy. In *Des Arts Diplomatiques. Les Cadeaux Diplomatiques Entre la Chine et l'Europe aux XVIIe-XVIIIe Siècles. Pratiques et Enjeux*; Zhao, B., Landry-Deron, I., Simon, F., Eds.; *Extrême-Orient Extrême-Occident* **2019**, *43*, 143–172.
11. Ma, H.J., Henderson, J.; Cui, J.F.; Chen, K.L. Glassmaking in the Qing Dynasty: A Review, New Data, and New Insights. *Adv. Archaeomater.*, **2020,** 1, pp. 27–35. https://doi.org/j.aia.2020.11.001
12. Curtis, E.B. Aspects of a multi-faceted process: The circulation of enamel wares between the Vatican and Kangxi's court. In *Des arts Diplomatiques. Les Cadeaux Diplomatiques Entre la Chine et l'Europe aux XVIIe-XVIIIe Siècles. Pratiques et Enjeux*; Zhao, B., Landry-Deron, I., Simon, F., Eds.; *Extrême-Orient Extrême-Occident* **2020**, *43*, pp. 29–39.
13. Xu, Y. Painted enamel on ceramics. The encounter on Dutch and Chinese pottery. https://www.aronson.com/painted-enamel-on-ceramic-the-encounter-of-dutch-and-chinese-pottery/ (accessed 9th November 2022)
14. Wang, M.C.-P. Eighteenth-century Chinese Painted Enamelware Materials and Technique, *Fondation Baur Bulletin* **2022**, *80*, 24-53.
15. Colomban, P.; Kırmızı, B.; Gougeon, C.; Gironda, M.; Cardinal, C. Pigments and glassy matrix of the 17th–18th century enamelled French watches: A non-invasive on-site Raman and pXRF study. *J. Cult. Herit.* **2020**, *44*, 1–14. https://doi.org/10.1016/j.culher.2020.02.001.
16. Shih, C.-F. The Arrival of a New Colour Palette in Eighteenth-century Jingdezhen. In Le Secret des couleurs – Céramiques de Chine et d'Europe du XVIIIe siècle à nos jours, d'Abrigeon, P. Ed. ; Fondation Baur-Musée des Arts d'Extrême-Orient, Genève, 2022, pp 20-59.
17. Colomban, P.; Milande, V.; Lucas, H. On-site Raman analysis of Medici porcelain, *J. Raman Spectrosc.* **2004**, *35[1],* 68-72. https://doi.org/10.1002/jrs.1085

18. Colomban, P.; Gironda, M.; Edwards, H.G.M.; Mesqui, V. The enamels of the first (softpaste) European blue-and-white porcelains: Rouen, Saint-Cloud and Paris factories: Complementarity of Raman and X-ray fluorescence analyses with mobile instruments to identify the cobalt ore. *J. Raman Spectrosc.* **2021**, *52*, 2246–2261. https://doi.org/10.1002/jrs.6111.
19. Wood, N. *Chinese Glazes: Their Origins, Chemistry and Recreation*; A & C Black: London, UK, 1999; pp. 194-195.
20. Kerr, R.; Wood, N. *Science and Civilisation in China: Volume 5, Chemistry and Chemical Technology*, Part 12, Ceramic Technology, Cambridge University Press: Cambridge, UK, 2004.
21. Wood, N. An AAS study of Chinese imperial yellow porcelain odies and their place in the history of Jingdezhen's porcelain development, *Adv. Archaeomater.* **2021**, *2(1)*, 49-65.
22. Colomban, P.; Treppoz, F. Identification and differentiation of ancient and modern European porcelains by Raman macro- and micro-spectroscopy. *J. Raman Spectrosc.* **2001**, *32*, 93–102. https://doi.org/10.1002/jrs.678.
23. Colomban, P.; Sagon, G.; Faurel, X. Differentiation of antique ceramics from the Raman spectra of their coloured glazes and paintings. *J. Raman Spectrosc.* **2001**, *32(5),* 351-360. DOI :10.1002/jrs.996
24. Colomban, P. Glazes and Enamels. In *Encyclopedia of Glass Science, Technology, History, and Culture*; Richet, P., Ed.; J. Wiley & Sons Inc., New York, 2020. Ch.10.6 https://www.wiley.com/en-us/Encyclopedia+of+Glass+Science%2C+Technology%2C+History%2C+and+Culture%2C+2+Volume+Set-p-9781118799499
25. Colomban, P. Glass, Pottery and enamelled objects: identification of their technology and origin, in *Conservation Science – Heritage Materials*, Ch. 7, P. Garside and E. Richarson Eds, The Royal Society of Chemistry, Cambridge, 2019, pp. 200-247. https://pubs.rsc.org/en/content/ebook/978-1-78801-093-1
26. d'Albis, A. *Traité de la Porcelaine de Sèvres*; Faton: Dijon, France, 2003.
27. d'Albis, A. Une remarquable tasse en rouge de cuivre réalisée à la Manufacture de Sèvres en 1848. In d'Abrigeon, P. Ed. Le Secret des Couleurs – Céramiques de Chine et d'Europe du XVIIIe siècle à nos jours. Fondation Baur-Musée des Arts d'Extrême-Orient, Genève, 2022, pp 131-135.
28. Maggetti, M.; d'Albis, A. Phase and compositional analysis of a Sèvres soft paste porcelain plate from 1781, with a review of early porcelain techniques. *Eur. J. Min.* **2017**, *29*, 347–367. https://doi.org/10.1127/ejm/2017/0029-2627.
29. Epler, R.A; Epler, D.R**.** *Glazes and glass coatings*, The American Ceramic Society: Westerville, OH, USA, 2000.
30. Fraser, H. *Glazes for the craft potter, Revised edition*, A&C Black: London, UK and The American Ceramic Society:Westerville, OH, USA
31. Colomban, P.; Milande, V. On-site Raman analysis of the earliest known Meissen porcelain and stoneware. *J. Raman Spectrosc.* **2006,** *37(5),* 606-613. DOI : 10.1002/jrs.1494
32. Munier, P. *Technologie des Faïences*, Gauthier-Villars, 1957, Paris.
33. Colomban, P.; Simsek Franci, G.; Kırmızı, B. Cobalt and Associated Impurities in Blue (and Green) Glass, Glaze and Enamel: Relationships between Raw Materials, Processing, Composition, Phases and International Trade. *Minerals* **2021**, *11(6),* 633. https://doi.org/10.3390/min11060633.
34. Neri, E.; Morvan, C.; Colomban, P., Guerra, M.F. Late Roman and Byzantine mosaic opaque 'glass-ceramics' tesserae (5th-9th century), *Ceram. Int.* **2016**, *42*, 18859-18869. https://doi.org/10.1016/j.ceramint.2016.09.033
35. Colomban, P.; Gironda, M.; Vangu, D.; Kırmızı, B.; Zhao, B.; Cochet, V. The technology transfer from Europe to China in the 17th–18th centuries: Non-invasive on-site XRF and Raman analyses of Chinese Qing Dynasty enameled masterpieces made using European ingredients/recipes. *Materials* **2021**, *14(23)*, 7434. https://doi.org/10.3390/ma14237434
36. Colomban, P.; Simsek Franci, G.; Gironda, M.; d'Abrigeon, P.; Schumacher, A.-C. pXRF Data Evaluation Methodology for On-site Analysis of Precious Artifacts: Cobalt used in the Blue Decoration of Qing Dynasty Overglazed Porcelain enameled at Custom District (Guangzhou), Jingdezhen and Zaobanchu (Beijing) workshops. *Heritage* **2022**, *5(3)*, 1752-1778. https://doi.org/10.3390/heritage5030091
37. Colomban, P.; Gironda, M.; Simsek Franci, G.; d'Abrigeon, P. Distinguishing Genuine Imperial Qing Dynasty Porcelain from Ancient Replicas by On-site Non-invasive XRF and Raman Spectroscopy, *Materials* **2022**, *15*, 5747. https://doi.org/10.3390/materials15165747.
38. Colomban, P.; Zhang, Y.; Zhao, B. Non-invasive Raman analyses of *huafalang* and related porcelain wares. Searching for evidence for innovative pigment technologies. *Ceram. Int.* **2017**, *43*, 12079–12088. https://doi.org/10.1016/j.ceramint.2017.06.063.
39. Colomban, P.; Kırmızı, B.; Zhao, B.; Clais, J.-B.; Yang, Y.; Droguet, V. Non-invasive on-site Raman study of pigments and glassy matrix of the 17th–18th century painted enamelled Chinese metal wares: Comparison with French enamelling technology. *Coatings* **2020**, *10*, 471. https://doi.org/10.3390/coatings10050471.
40. Colomban, P.; Gironda, M.; Vangu, D.; Kırmızı, B.; Zhao, B.; Cochet, V. The technology transfer from Europe to China in the 17th–18th centuries: Non-invasive on-site XRF and Raman analyses of Chinese Qing Dynasty enameled masterpieces made using European ingredients/recipes. *Materials* **2021**, *14*, 7434. https://doi.org/10.3390/ma14237434.

41. Colomban, P.; Ngo, A.-T.; Fournery, N. Non-invasive Raman Analysis of 18th Century Chinese Export/Armorial Overglazed Porcelain: Identification of the Different Enameling Technology. *Heritage* **2022**, *5*, 233–259. https://doi.org/10.3390/heritage5010013.
42. Colomban, P.; Ambrosi, F.; Ngo, A.-T.; Lu, T.-A.; Feng, X.-L.; Chen, S.; Choi, C.-L. Comparative analysis of *wucai* Chinese porcelains using mobile and fixed Raman microspectrometers. *Ceram. Int.* **2017**, *43*, 14244–14256. https://doi.org/10.1016/j.ceramint.2017.07.172.
43. Colomban, P.; Kırmızı, B.; Zhao, B.; Clais, J.-B.; Yang, Y.; Droguet, V. Investigation of the Pigments and Glassy Matrix of Painted Enamelled Qing Dynasty Chinese Porcelains y Noninvasive On-Site Raman Microspectrometry, *Heritage* **2020**, *3, 915-941*. https://doi.org/10.3390/heritage3030050.
44. Simsek Franci, G. Blue Print: Archaeometric Studies of Colored Glazed Chinese Ceramics and Production of Replica, Final Report, The Scientific and Research Council of Turkey, The Scientific and Technological Projects Funding Program. Unpublished Report, 3 January 2021.
45. Simsek Franci, G. Handheld X-ray Fluorescence (XRF) versus wavelength dispersive XRF: Characterization of Chinese blue and white porcelain sherds using handheld and laboratory-type XRF instruments. *Appl. Spectrosc.* **2020**, *74*, 314–322.
46. Simsek, G.; Colomban, P.; Wong, S.; Zhao, B.; Rougeulle, A.; Liem, N.Q. Toward a fast non-destructive identification of pottery: The sourcing of 14th-16th century Vietnamese and Chinese ceramic shards. *J. Cult. Herit.* **2015**, *16*, 159–172. https://doi.org/10.1016/j.culher.2014.03.003.
47. Liu, H.W.; Wang, H.;Duan, P.Q.; Gao, H.; Zhang, R.; Qu, L. The Qianlong Emperor's order: scientific analysis helpsfind French painted enamel among Palace Museum collections, *Heritage Sci.* **2022**, *10*, 132. https://doi.org/10.1186/s40494-022-00764-9
48. Kingery, W.D.; Vandiver, P.B. The Eighteenth-Century Change in Technology and Style from the *Famille-Verte* Palette to the *Famille-Rose* Palette. In *Technology and Style*; Kingery, W.D., Ed.; Ceramics and Civilization Series, Vol. 2, The American Ceramic Society: Colombus, USA, 1986, pp. 363–381.
49. Van Pevenage, J.; Lauwers, D.; Herremans, D.; Verhaeven, E.; Vekemans, B.; de Clercq, W.; Vincze, L.; Moens, L.; Vandenabeele, P. A combined spectroscopic study on Chinese porcelain containing ruan-cai colours, *Anal. Meth.* **2014**, 6387–6394.
50. Li, Y.Q.; Zhu, J.; Ji, L.Y.; Shan,Y.Y.; Jiang, S.; Chen, G.; Sciau, P.; Wang, W.X.; Wang, C.S. Study of Arsenic in *Famille Rose* Porcelain from the Imperial Palace of Qing Dynasty, Beijing, China. *Ceram. Int.* **2018**, *44*, 1627–1632. https://doi.org/10.1016/j.ceramint.xxxxx
51. Duan, H.Y., Zhang, X.Q.; Kang, B.Q.; Wang,G.Y.; Qu, L.; Lei, Y. Non-Destructive Analysis and Deterioration Study of a Decorated *Famille Rose* Porcelain Bowl of Qianlong Reign from the Forbidden City. *Stud. Conserv.* **2019**, *64(6)*, 311–322.
52. Giannini, R.; Freestone, I.C.; Shortland, A.J. European cobalt sources identified in the production of Chinese *famille rose* porcelain. *J. Archaeol. Sci.* **2017**, *80*, 27–36.
53. Wang, Q.; Chin, L.; Wang, C. *Underglaze Blue and Red: Elegant Decoration on Porcelain of Yuan, Ming and Qing*; Multi-Art: Hong Kong, 1993.
54. Norris, D. E.; Braekmans, D.; Domoney, K.; Shortland, A. The Composition and Technology of Polychrome Enamels on Chinese Ruby-Backed Plates Identified Through Nondestructive Micro-X-Ray Fluorescence. *X-Ray Spectrometry* **2020**, *49(4),* 502–510.
55. Miao, J.; Yang B.; Mu D. 2010. Identification and Differentiation of Opaque Chinese Overglaze Yellow Enamels by Raman Spectroscopy and Supporting Techniques. *Archaeometry* **2020**, *52(1)*, 146–155.
56. Norris, D. E.; Braekmans, D.; Shortland, A. Technological connections in the development of 18th and 19th century Chinese painted enamels, *J. Archaeol. Sci.: Reports* **2022**, *42*, 103406. https://doi.org/J.jasrep.2022.103406
57. Burlot,J.; Colomban, P.; Bellot-Gurlet, L.; Lemasson, Q. PIGE and PIXE evidence of the use of lithium-rich borax in Chinese and European 18th century enamel, to be published.
58. Menegon, E. Amicia Palatina: les jésuites et la politique des cadeaux offerts à la Cour de Qing, *Extrême-Orient Extrême-Occident* **2019**, *43*, 61-80.
59. Deck, T. *La faïence*, Maison Quantin:Paris, France, 1887.
60. d'Abrigeon, P. Ed. *Le Secret des Couleurs – Céramiques de Chine et d'Europe du XVIIIe siècle à nos jours*. Fondation Baur-Musée des Arts d'Extrême-Orient, Genève, 2022.
61. Tang, H. Colour Matters: The Consumption of Overglaze enameled Wares in Eighteenth-century Europe. In *Le Secret des Couleurs – Céramiques de Chine et d'Europe du XVIIIe siècle à nos jours*. d'Abrigeon, P. Ed. Fondation Baur-Musée des Arts

668 d'Extrême-Orient, Genève, 2022.
669 62. Jörg, C.J.A. *Porcelain and the Dutch China Trade*, La Haye, Martinus Nijhoff, 1982.
670 63. Scott, R.E. Ed. *Chinese Copper Red Wares*, London, Percival David Foundation of Chinese Art, 1992.
671 64. National Palace Museum, ed., 1992, *Special Exhibition of Ch'ing Dynasty Enamelled Porcelains of the Imperial Ateliers*, National Pal-
672 ace Museum: Taipei, Taiwan.
673 65. Cort, L.A. Stuart J. *Joined Colors: Decoration and Meaning in Chinese Porcelain*, Whashington D.C./Hong Kong, Arthur M. Sackler
674 Gallery, Smithsonian Institution/Tai Yip Co. 1993.
675 66. Shih, C.-F. *Hua Falang: The Chinese Concept of Painted Enamels, in the RA Collections of Chinese Ceramics: A Collector's Vision*, vol. V,
676 London, Jorge Welsh Books, 2001, pp 29-59.
677 67. Shih, C.-F. *Radiant Luminance: the Painted Enamelware of the Qing Imperial Court*, Taipei, The national Palace Museum, 2012.
678 68. Kleutghen, K., Chinese Occidenterie: the Diversity of "Western" Objects in Eighteenth-Century China, *Eighteenth-Century*
679 *Studies* **2014**, *47(2),* 117-35. https://openjournals.nl/the-rijksmuseum-bulletin/article/download/9836/10332/16235 (Accessed
680 20th October 2021)
681 69. Palace Museum ed., *Treasures from Oversea Countries, Exhibition Catalogue of Kulangsu Gallery of Foreign Artefacts from the Palace*
682 *Museum Collection*. Gugong chubanshe: Beijing, PRC, 2011.
683 70. Available online: https://xrfcheck. bruker.com/InfoDepth (accessed on 6 July 2022).
684 71. Sakellariou, K.; Miliani, C.; Morresi, A.; Ombelli, M. Spectroscopic investigation of yellow majolica glazes. *J. Raman Spectrosc.*
685 **2004,** *35*, 61–67.
686 72. Sandalinas, C.; Ruiz-Moreno, S. Lead-tin-antimony yellow-Historical manufacture, molecular characterization and identifica-
687 tion in seventeenth-century Italian paintings. *Stud. Conserv*. **2004**, *49*, 41–52.
688 73. Sandalinas, C.; Ruiz-Moreno, S.; Lopez-Gil, A.; Miralles, J. Experimental confirmation by Raman spectroscopy of a Pb-Sn-Sb
689 triple oxide yellow pigment in sixteenth-century Italian pottery. *J. Raman Spectrosc.* **2006,** *37*, 1146–1153.
690 74. Rosi, F.; Manuali, V.; Miliani, C.; Brunetti, B.G.; Sgamellotti, A.; Grygar, T.; Hradil, D. Raman scattering features of lead
691 pyroantimonate compounds. Part I: XRD and Raman characterization of $Pb_2Sb_2O_7$ doped with tin and zinc. *J. Raman Spectrosc*.
692 **2009**, *40*, 107–111.
693 75. Ricciardi, P.; Colomban, P.H.; Tournié, A.; Milande, V. Non-destructive on-site identification of ancient glasses: Genuine arte-
694 facts, embellished pieces or forgeries? *J. Raman Spectrosc.* **2009**, *40*, 604–617.
695 76. Pereira, M.; de Lacerda-Aroso, T.; Gomes, M.J.M.; Mata, A.; Alves, L.C.; Colomban, P.H. Ancient Portuguese ceramic wall tiles
696 ("Azulejos"): Characterization of the glaze and ceramic pigments. *J. Nano Res.* **2009**, *8*, 79–88.
697 77. Pelosi, C.; Agresti, G.; Santamaria, U.; Mattei, E. Artificial yellow pigments: Production and characterization through spectro-
698 scopic methods of analysis. *e-Preserv. Sci.* **2010**, *7*, 108–115.
699 78. Rosi, F.; Manuali, V.; Grygar, T.; Bezdicka, P.; Brunetti, B.G.; Sgamellotti, A.; Burgio, L.; Seccaroni, C.; Miliani, C. Raman scat-
700 tering features of lead pyroantimonate compounds: Implication for the non-invasive identification of yellow pigments on an-
701 cient ceramics. Part II. In situcharacterisation of Renaissance plates by portable micro-Raman and XRF studies. *J. Raman*
702 *Spectrosc.* **2011**, *42*, 407–414.
703 79. Cartechini, L.; Rosi, F.; Miliani, C.; D'Acapito, F.; Brunetti, B.G.; Sgamellotti, A. Modified Naples yellow in Renaissance majoli-
704 ca: Study of Pb-Sb-Zn and Pb-Sb-Fe ternary pyroantimonates by X-ray absorption spectroscopy. *J. Anal. At. Spectrom*. **2011**, *26*,
705 2500–2507.
706 80. Pinto, A.; Sciau, P.; Zhu, T.Q.; Zhao, B.; Groenen, E.S. Raman study of Ming porcelain dark spots: Probing Mn-rich spinels. *J.*
707 *Raman Spectrosc.* **2019,** *50*, 711–719. https://doi.org/10.1002/jrs.5568.
708 81. Porter, Y. Le cobalt dans le monde Iranien (IXe-XVIe siècles). *Taoci* **2000**, *1*, 5–14.
709 82. Matin, M.; Pollard, A.M. From ore to pigment: A description of the minerals and experimental study of cobalt ore processing
710 from the Kâshân mine, Iran. *Archaeometry* **2017**, *59*, 731–746, doi:10.1111/arcm.12272.
711 83. Matin, M.; Pollard, A.M. Historical accounts of cobalt ore processing from the Kāshān mine, Iran. *Iran* **2015**, *53*, 171–183.
712 84. Watt, J.C.Y. Notes on the use of cobalt in later Chinese ceramics. *Ars Orient.* **1979**, *11*, 63–85.
713 85. Wen, R.; Wang, C.S.; Mao, Z.W.; Huang, Y.Y.; Pollard, A.M. The chemical composition of blue pigment on Chinese
714 blue-and-white porcelain of the Yuan and Ming Dynasties (AD 1271–1644). *Archaeometry* **2007**, *49*, 101–115.
715 86. Huang, S.-Z. *Xi Yang Chao Gong Dian Lu (Registration of Taxes from Foreign Countries*), Zhong wai jiao tong shi ji cong kan Series;
716 1520. (in Chinese)
717 87. Medley, M. *The Chinese Potter. A Practical History of Chinese Ceramics, 3rd ed.*; Phaidon, London, UK, 1999**.**
718 88. Yu, K.N.; Miao, J.M. Non-destructive analysis of Jingdezhen Blue and White porcelains of the Ming dynasty using EDXRF.
719 *X-ray Spectrometry*, **1996**, *25*, 281–285.

89. Colomban, P.; Liem, N.Q.; Sagon, G.; Tinh, H.X.; Hoành, T.B. Microstructure, composition and processing of 15th century Vietnamese porcelains and celadons. *J. Cult. Herit.* **2003**, *4*, 187–197.
90. Yap, C.T.; Tang, S.M. X-ray fluorescence analysis of modern and recent Chinese porcelains. *Archaeometry* **1984**, *26*, 78–81.
91. Yap, C.T. A quantitative spectrometric analysis of trace concentrations of manganese and cobalt in ceramics and the significance of As/Co and Mn/Co ratios. *J. Archaeol. Sci.* **1988**, *15*, 173–177.
92. Yu, K.N.; Miao, J.M. Locating the origins of blue and white porcelains using EDXRF. *Appl. Radiat. Isot.* **1997**, *48*, 959–953.
93. Yu, K.N.; Miao, J.M. Multivariate analysis of the energy dispersive X-ray fluorescence results from blue and white Chinese porcelains. *Archaeometry*, **1998**, *40*, 331–339, doi:10.1111/j.1475-4754.1998.tb00841.x.
94. Yu, K.N.; Miao, J.M. Characterization of blue and white porcelains using Mn/Fe ratio from EDXRF, with particular reference to porcelains of the Xuande period (1426 to 1435 A.D.). *Appl. Radiat. Isot.* **1999**, *51*, 279–283, doi:10.1016/S0969-804300059-7.
95. Morimoto, A.; Yamasaki, K. *Technical Studies on Ancient Ceramics Found in North and Central Vietnam*; Fukuoka Museum: Fukuoka, Japan, 2001.
96. Cheng, H.S.; Zhang, B.; Xia, H.N.; Jiang, J.C.; Yang, F.J. Non-destructive analysis and appraisal of ancient Chinese porcelain by PIXE. *Nucl. Instr. Meth. Phys. Res. Sect. B* **2002**, *190*, 488–491, doi:10.1016/S0168-583X01280-0.
97. Colomban, P.; Calligaro, T.; Viert-Guigue, C.; Nguyen, N.Q.; Edwards, H.G.M. Dorures des céramiques et tesselles anciennes: technologies et accrochage. *ArchéoSciences* **2005**, *29*, 7-20.
98. Bertran, H.; Reboulleau; Magnier; Romain, A. *Nouveau Manuel Complet de la Peinture sur Verre, sur Porcelaine et sur Émail*; Encyclopédie-Roret, L. Mulo: Paris, France, 1913.
99. Simsek, G.; Colomban, P.; Casadio, F.; Bellot-Gurlet, L.; Zelleke, G.; Faber, K.T.; Milande, V.; Tilliard, L. On-site Identification of Early Böttger Red Stoneware using portable XRF/Raman Instruments: 2, Glaze and Gilding Analysis, *J. Am. Ceram. Soc.* **2015**, *98(10)*, 3006-3013. https://doi.org/10.1111/jace.13720.
100. Demirsar Arli, B.; Simsek Franci, G.; Kaya, S.; Arli, H.; Colomban, P. Portable X-ray Fluorescence (p-XRF) uncertainty estimation for glazed ceramic analysis: Case of Iznik Tiles. *Heritage* **2020**, *3*, 1302–1329; doi:10.3390/heritage3040072.
101. Colomban, P. The Discovery and Comparison of the Manufacturing Secrets of Enamelled Masterpieces, *Orientations* **2022**, *53(1)*, 92-96.
102. Zhang, F.K. The origin and development of traditional Chinese glazes and decorative ceramics color. In Kingery W.D. Ed. Vol. 1 *Ancient Technology to Modern Science, Ceramics and Civilization*, The American Ceramic Society, Westerville, 1984, pp. 163-180.
103. Yang, Y.M.; Feng, M.; Ling, X.; Mao, Z.Q.; Wang, C.S.; Sun, X.M.; Guo, M. Microstructural analysis of the color-generating mechanism in Ru ware, modern copies and its differentiation with Jun ware. *J. Archaeol. Sci.* **2005**, *32*, 301-310.
104. Kingery, W.D.; Vandiver, P.B. Song Dynasty Jun (Chung) ware glazes. *Am. Ceram. Bull.* **1983**, *62*, 1269-1274.
105. Freestone, I.C.; Barber, D.J. The development of the colour of sacrificial red glaze with special reference to a Qing Dynasty saucer dish, in *Chinese Copper Red Wares*. Scott R.E. Ed. Percival David Foundation of Chinese Art, Monograph Series n°3, University of London, School of Oriental and African Art, London, 1992, pp 53-62.
106. Sciau, P.; Noé, L. Colomban, P. Metal nanoparticles in contemporary potters' master pieces: Lustre and red 'pigeon lood' potteries as models to understand the ancient pottery, *Ceram. Int.* **2016**, *42*, 15349-15357. https://doi.org/10.1016/j.ceramint.2016.06.179
107. Hunt, L. B.Gold in the Pottery Industry. The history and Technology of Gilding Processes. Gold Bull. **1979**, *12(3)*, 116-127.
108. Colomban, P. The Use of Metal Nanoparticles to Produce Yellow, Red and Iridescent Colour, from bronze Age to Present Times in Lustre Pottery and Glass: Solid State Chemistry, Spectroscopy and Nanostructure. *J. Nano Res.* **2009**, *8*, 109–132.
109. Geyssant, J. *Secret* du verre rouge transparent de *Bernard Perrot* et comparaison avec celui de Johann Kunckel. In *Bernard Perrot (1640–1709), Secrets et Chefs-d'œuvre des Verreries Royales d'Orléans, Catalogue*; Klinka Ballesteros, I., de Valence, C., Maitte, C., Ricke, H., Eds.; Musée des Beaux-Arts d'Orléans—SOMOGY Editions d'Arts: Paris, France, 2013; pp. 51–54.
110. Colomban, P.; Kırmızı, B. Non-invasive on-site Raman study of polychrome and white enamelled glass artefacts in imitation of porcelain assigned to Bernard Perrot and his followers. *J. Raman Spectrosc.* **2020**, *51*, 133–146.
111.

1. Author 1, A.B.; Author 2, C.D. Title of the article. *Abbreviated Journal Name* **Year**, *Volume*, page range.
2. Author 1, A.; Author 2, B. Title of the chapter. In *Book Title*, 2nd ed.; Editor 1, A., Editor 2, B., Eds.; Publisher: Publisher Location, Country, 2007; Volume 3, pp. 154–196.
3. Author 1, A.; Author 2, B. *Book Title*, 3rd ed.; Publisher: Publisher Location, Country, 2008; pp. 154–196.
4. Author 1, A.B.; Author 2, C. Title of Unpublished Work. *Abbreviated Journal Name* year, *phrase indicating stage of publication (submitted; accepted; in press)*.
5. Author 1, A.B. (University, City, State, Country); Author 2, C. (Institute, City, State, Country). Personal communication, 2012.
6. Author 1, A.B.; Author 2, C.D.; Author 3, E.F. Title of Presentation. In Proceedings of the Name of the Conference, Location of Conference, Country, Date of Conference (Day Month Year).
7. Author 1, A.B. Title of Thesis. Level of Thesis, Degree-Granting University, Location of University, Date of Completion.
8. Title of Site. Available online: URL (accessed on Day Month Year).